Bio-Design and Manufacturing (2023) 6:340–371
https://doi.org/10.1007/s42242-023-00232-8

REVIEW

# Mechanical stimulation devices for mechanobiology studies: a market, literature, and patents review

F. Melo-Fonseca[1,2,3] · O. Carvalho[1,2] · M. Gasik[4,5] · G. Miranda[6] · F. S. Silva[1,2]

Received: 2 April 2022 / Accepted: 8 January 2023 / Published online: 1 April 2023


## Abstract

Significant advancements in various research and technological fields have contributed to remarkable findings on the physiological dynamics of the human body. To more closely mimic the complex physiological environment, research has moved from two-dimensional (2D) culture systems to more sophisticated three-dimensional (3D) dynamic cultures. Unlike bioreactors or microfluidic-based culture models, cells are typically seeded on polymeric substrates or incorporated into 3D constructs which are mechanically stimulated to investigate cell response to mechanical stresses, such as tensile or compressive. This review focuses on the working principles of mechanical stimulation devices currently available on the market or custom-built by research groups or protected by patents and highlights the main features still open to improvement. These are the features which could be focused on to perform, in the future, more reliable and accurate mechanobiology studies.

## Graphic abstract

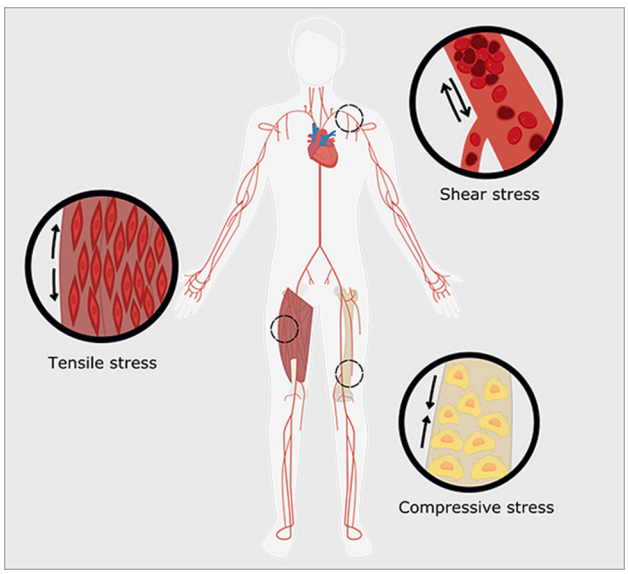


**Keywords** Biomaterials · Polymers · Actuators · Mechanical stress · Mechanotransduction

## Contextualization

The adult human body is composed of approximately 37 trillion cells, all synchronized to maintain equilibrium [1]. Cells reside in a complex and dynamic microenvironment containing biological, chemical, physical, and mechanical

G. Miranda and F. S. Silva have contributed as co-last authors.

✉ F. Melo-Fonseca
franciscarmelofonseca@gmail.com

Extended author information available on the last page of the article

cues which often regulate cell proliferation, migration, differentiation, and function, and ultimately, may be responsible for the development of disease [2]. To study and understand how cells respond to mechanical stimuli or how host cells will behave upon the implantation of biomaterials, researchers use mechanical stimulation devices. These devices subject biomaterials to a particular mechanical stress with the aim of stimulating cells through deformation of the biomaterials. Devices which are currently commercially available offer limited customization and restricted force measurement capabilities [3, 4]. As a consequence, a wide variety of apparatuses, with varying levels of sophistication, design, functionality, and precision, have been custom-built by research groups to meet particular needs, while others are protected by patents. This review focuses on the working principles, functionality, and main operational features of a number of mechanical stimulation devices developed over the past years, and highlights the main features still open to improvement.

## The cellular microenvironment

All cells are in permanent interaction with the surrounding microenvironment, including the extracellular matrix (ECM) and neighbouring cells. That interaction is based on a combination of multiple cues, including biological and physical cues able to influence cell behaviour [5, 6]. Cells are constantly and cyclically subjected to external forces whose type and magnitude are highly variable and dependent on location [7]. These forces are crucial from the beginning of cell life: throughout the development of embryos, and in everyday activities, in which cells experience shear stress during breathing and blood flow, or tensile and compressive stresses from skeletal muscle contraction, joint loading, and tendon/ligament stretching [8–11]. Their ability to sense externally imposed forces and mechanical properties of the surrounding ECM is denominated "cell mechanosensing" [12]. These signals are later converted into changes in intracellular biochemistry and gene expression, a process often referred to as "mechanotransduction" [13]. Mechanical stimuli include not only externally imposed forces (namely tensile, compressive, and shear forces), but also intrinsic cellular tensions generated by active cell contraction [7]. In fact, besides the intracellular response to dynamic modifications of the ECM, cells are also able to influence the environment, leading to a reciprocal interaction [7, 11]. Both outside-in and inside-out pathways exist in mechanotransduction processes, and are able to trigger signalling cascades [14, 15]. In this sense, the environment plays an important role in many cellular processes, such as cellular adhesion, migration, proliferation, differentiation, and apoptosis [15]. Given the importance of mechanical interactions in cellular behaviour, mechanobiology has emerged as a novel interdisciplinary field combining biology, mechanics, and engineering, which aims to understand how cells sense and behave in response to mechanical stimuli [7, 11, 16, 17]. Over the past few decades, researchers have developed systems to control the cellular microenvironment and, while some focus on improving cell culture conditions, others aim to study the effects of a particular mechanical stimulus on cells by using unique cells or biomaterial-based constructs.

## Moving from 2D to 3D models

Biological systems are organized into several levels of structural organization, becoming more complex as the length scale increases. Beginning at the micrometre scale, cells assemble to form tissues, which are organized into organs, which together form the organism, the highest level of organization, on the metre scale. Biological model systems range from simplified two-dimensional (2D) cell cultures to more complex three-dimensional (3D) cell cultures, organoids, tissue explants, and model organisms, such as the mouse [2]. As the complexity rises, the associated cost and physiological relevance increase, while experimental accessibility decreases [2].

The 2D and 3D cell culture systems discussed below are illustrated in Fig. 1, in both static and dynamic modes. In conventional and static cell cultures, the nutrient supply is maintained by frequently changing the culture medium. Primary cells or established cell lines may be cultured as a 2D monolayer, in the case of an adherent culture, or as a cell suspension known as a "suspension culture". Although monolayer cultures are easily manipulated, used worldwide in life-science research, and still accepted as the gold standard, cells are highly anisotropic. This is why it has been experimentally observed that even within a particular cell line, cellular responses may differ for an identical mechanical input [18]. Moreover, it has been reported that cells may lose some differentiated characteristics [19] and that conventional 2D culture models, whether in Petri dishes or culture flasks, do not replicate the dynamic in vivo 3D microenvironment [2]. As a consequence, over the past decades, researchers have focused on more complex cell culture models which include cell seeding on prefabricated scaffolds or incorporate cells into 3D scaffolds (usually hydrogels made of synthetic polymers). These materials allow cellular spatial organization into functional cell-based constructs. In order to keep up with continuously more complex and demanding research, bioreactor systems were developed for numerous applications, for example, in the context of cell biology research and regenerative medicine therapies. While the absence of media mixing or circulation in a static aqueous environment leads to limited diffusion of fluids or

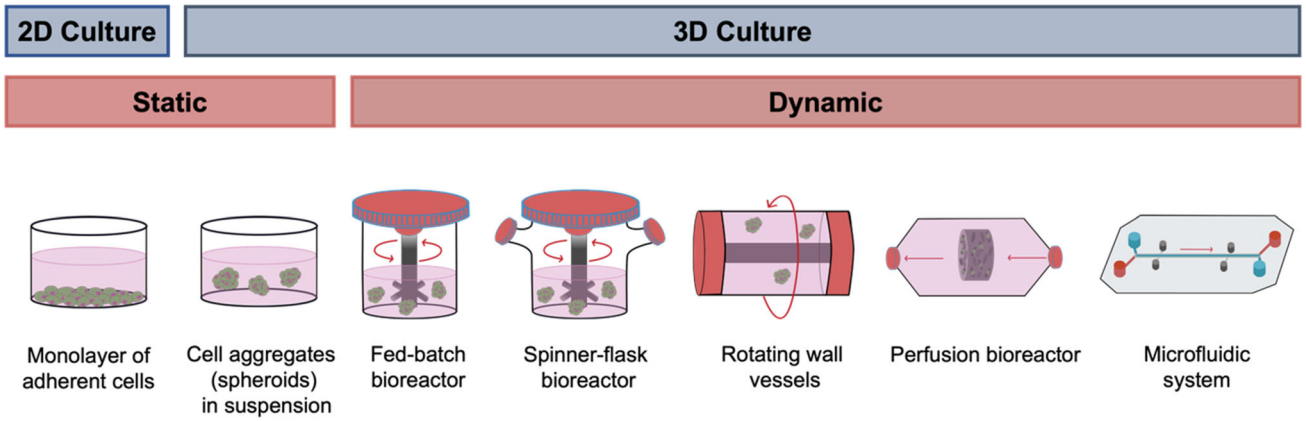


**Fig. 1** Cell culture models may be in a static or dynamic mode. In 2D monolayer cultures, adherent cells are in contact with the culture vessel, neighbouring cells, and the culture medium. In non-adherent plates, 3D spheroids are grown in suspension, either without or with medium agitation (fed-batch bioreactor). In spinner-flask bioreactors, cell dispersion or cell-based constructs attached to a needle are in contact with a homogeneous medium due to agitation and medium perfusion. Rotating wall vessels enable cell culture mixing without an internal stirring mechanism by definition of a proper rotation speed. Perfusion bioreactors use continuous and fresh medium perfusion through cell-based constructs, provided by peristaltic pumps. Microfluidic systems are used for culturing and monitoring of both adherent and non-adherent cells. The fluid dynamics is represented by the red arrow

gases and contributes to cell-waste accumulation and nutrition depletion [5, 20], 3D models with continuously mixed media in a dynamic culture allow homogeneous media and cell dispersion, better reproducing the in vivo spatial and biomechanical complexity [19]. Three-dimensional culture systems, particularly bioreactors, are not the scope of this review, but extensive works on this topic may be easily found in the literature [2, 20–23]. Briefly, fluid-flow-induced bioreactors are designed to enhance nutrient supply to cell cultures and replicate tissue-specific conditions [24]. They are often grouped into fed-batch [25], spinner-flask [26], rotating [24, 27], and perfusion bioreactors [21, 28]. Despite the continuous media agitation in bioreactors, an efficient supply of gases and nutrients is not always assured and sample handling and maintenance of sterility are challenging. Because of the constraints related to bioreactor size, cost, and time consumption when running parallel multiple experiments, the reactor volumes in microfluidic systems can be reduced down to picolitres, while assuring a laminal-flow pattern [29, 30]. In addition to the decrease in reagent consumption, the culture environment is particularly controlled, because cell shape, dimensionality, and density are tightly regulated in 10–100 μm channels [31, 32]. In the category of micro-engineered devices, lab-on-a-chip-based devices are commonly used for point-of-care diagnostics and are characterized by easy handling and high performance of body fluid analyses [33]. Organ-on-a-chip devices can be used for culturing cells, spheroids, organoids, and tissue biopsies and, among their final applications, can be used for drug screening and development, disease modelling, and the study of human physiology, due to their capability of closely replicating the dynamic microenvironment of living organs [30, 34]. However, the resultant fluid-flow-induced shear stresses may induce cell damage, and current devices lack automation and well-defined protocols [34]. In contrast to bioreactors, microfluidic-based culture models (or bioreactors on a chip) offer optimized culture conditions and precise control over the chemical and physical cellular environment through the integration of sensors [29].

Two-dimensional culture models are based on a cell monolayer in which cells are forced to adapt to an artificial, flat, and rigid surface [27], and thus do not provide meaningful information regarding the real dynamics that living cells and tissues experience. Therefore, 3D culture models have greatly increased in number and sophistication, and have the capability of more closely replicating the dynamic microenvironment. They are also more experimentally tractable than model organisms. Despite the fact that bioreactors and microfluidic-based platforms are attractive devices for transporting nutrients and thus improving overall cell culture conditions [2, 35], fluid-flow-induced shear stresses cannot be measured in this setting; thus, although this shear stress is considered an important contribution to cell metabolism, it cannot be considered as a mechanical input for mechanotransduction studies.

In the context of mechanobiology, external force can be applied through direct methods such as micropipette aspiration [36–38], atomic-force microscopy [38–41], and substrate deformation [32, 42–44]. Indirect methods can also be used, in which cells are, for example, subjected to optical or magnetic fields [45–47]. In direct methods, a generated

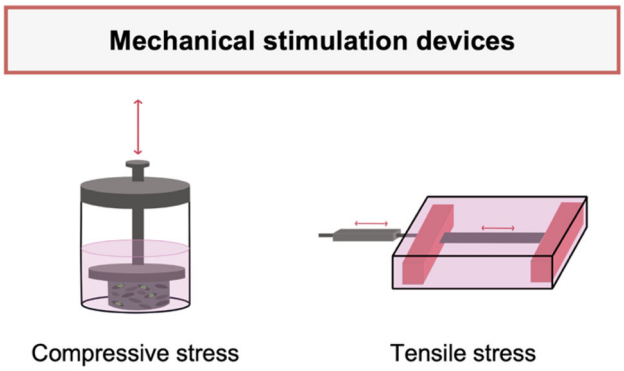


**Fig. 2** Examples of mechanical stimulation devices used for mechanobiology studies. The commonly studied mechanical stresses are compressive and tensile stresses, either applied to cells incorporated inside 3D constructs (left) or cells seeded on a flexible substrate (right). The movement imposed on the biomaterials is represented by the red arrow

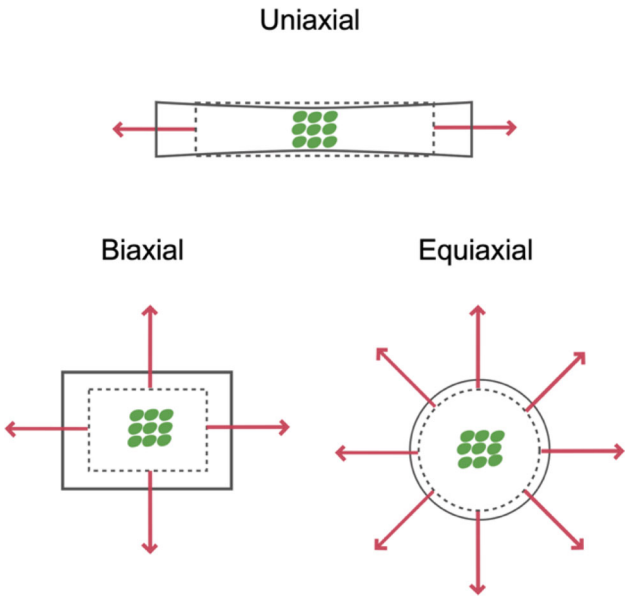


**Fig. 3** The substrate on which cells (represented by green circles) are cultured may be subjected to different strain modes: uniaxial, biaxial, or equiaxial, as a consequence of substrate movement imposed by the load

and controlled force is applied directly on cells, leading, in some cases, to a large global cell strain. On the other hand, indirect methods allow researchers to monitor deformation in different regions of a cell, but not to precisely control or measure the applied stress [32, 47].

Mechanical stimulation devices have been developed to study cellular response to an externally applied mechanical stimulus or to mimic physiological dynamics to perform more reliable studies. For example, one can apply compressive or tensile forces on cells in a controlled way via biomaterials, as illustrated in Fig. 2. Typically, these devices consist of a culture medium vessel, a specific space for the cell-based construct/substrate, and clamping parts to apply tensile or compressive loading in a controlled computed way [21]. Furthermore, some devices allow real-time monitoring by the use of chambers composed of light-transparent materials and multi-chamber configurations for parallel experiments [21]. Individual components, such as biomaterials, ECM, and soluble and mechanical cues, may be integrated in these systems to closely mimic the in vivo environment and study physiology and screen therapeutics.

## Emerging mechanical stimulation devices

Mechanical stimulation devices have gained interest due to their potential for replicating mechanical cues observed in the in vivo microenvironment, controlling mechanical and physical properties with precision, and in some cases, allowing simultaneous analysis [48, 49]. Mechanical strains in a given material obtained by applying either tensile or compressive stresses in any direction and at controlled loading features, such as strain magnitude and frequency, create a mechanical strain environment around the cultured cells. The strain profile obtained by such substrate deformation may occur in one of the three different modes illustrated in Fig. 3.

Novel and more complex devices have been developed to assure optimal cellular conditions during manipulation (e.g., application of a particular mechanical stimulus) and analyse the corresponding cellular behaviour in small-scale volumes. Some of the operational features of these mechanical stimulation devices are summarized in Table 1.

Depending on the goal of a particular study and consequently of the experimental design, cells may be seeded directly on the substrate or incorporated in functional constructs. Scaffolds or cell-based constructs are 3D structures often used to regulate the environment of cells, and in this sense, cells can be manipulated by controlling the mechanical properties of the scaffold, such as elasticity, rigidity, and strain. Natural scaffolds are made of naturally derived materials, namely collagen, fibrin, and components of decellularized tissues, whereas fully synthetic matrices are often composed of poly(dimethylsiloxane) (PDMS) and poly(L-lactide-co-glycolide) (PLGA) [27]. One of the most common materials used in mechanobiology research is PDMS, because it is non-cytotoxic, autoclavable, and flexible. Furthermore, it has high optical transparency and low auto-fluorescence, which allows cell analysis by fluorescence and optical imaging techniques [7, 50]. Hydrogels are biocompatible and biomimetic 3D structures which, once again, facilitate imaging because the cellular behaviour in their interior can be monitored. Moreover, hydrogels are typically used

**Table 1** List of operational features of mechanical stimulation devices

| Device feature | Description |
|---|---|
| Mechanical stimulus type | Selection depends on the study focus/application and may include at least one of the following: tensile, compressive, shear, or vibration stimulus |
| Definition of loading features | Strain mode (uniaxial, biaxial, or equiaxial), magnitude, frequency (static, cyclic, or intermittent), duration, and waveform (static, sinusoidal, ramp) |
| Aseptic conditions | The device parts in contact with the cell culture medium and/or cells must be sterile during sample handling and throughout the experiment |
| Incubation | - Short vs. long-term experiments<br>- The device either incorporates a means of changing the cell culture medium every few days, as well as controlling and maintaining the temperature at 37 °C, exchanging gases, and controlling humidity to perform long-term experiments (over more than 24 h), or has the correct geometry and dimensions to fit the incubator<br>- Static vs. dynamic culture (with or without continuous media mixing) |
| Multi-sample testing | Study more than one sample simultaneously (run in parallel more than one experiment) |
| Live imaging | Control and monitor cell behaviour in real time through glass or a transparent material, mostly by inverted confocal microscopy analysis |
| Automation | The drive mechanism may be automated |
| Maintenance | The device requires either low or high maintenance |

to apply mechanical stimuli on cells because they allow a uniform distribution of stresses throughout the structure [21].

One of the most important concerns in mechanobiology studies is to ensure aseptic conditions during experiments. Therefore, all parts of the mechanical stimulation device are assembled inside a laminal-flow biosafety cabinet and then the complete and mounted device along with its electronic components is placed in a typical culture incubator, allowing maximally sterile conditions and, when required, a long-term experiment. As already mentioned, confocal imaging is often preferable to upright microscopy techniques, mainly to overcome issues related to device size constraints. Therefore, the design of some devices considers the overall device dimensions to ensure that it fits in the microscope chamber, and the incorporation of a glass coverslip or other materials with similar optical properties to allow high-magnification imaging of the cultured or encapsulated cells, for example, for performing live imaging studies [32, 42, 51, 52]. Other developments are intended to produce high-throughput capabilities, such as by increasing the number of wells/chambers which can be loaded simultaneously [51, 53–57].

## Commercially available cell-stimulation devices

In vitro mechanical stimulation devices have been developed to apply specific mechanical stimuli to biomaterials and, in this way, stimulate cells, for example, as they would be stimulated by external cues typically observed in physiological conditions. Some tension and compression devices are available on the market, and the most well-known companies are FLEXCELL International Corporation, TA Instruments, CellScale, IonOptix, BISS, and Strex. Some features of their commercially available products, including the type of mechanical stimulus and the maximum strain and frequency that can be applied, are summarized in Table 2. Figure 4 is a graphical representation of the maximum strain/displacement and frequency provided by the device models.

Some of the commercialized devices may be used to evaluate a variety of specimens, including cells seeded in monolayers, 3D cell-seeded constructs (e.g. hydrogels), natural tissues, or bioartificial tissue samples. Stretching devices commercialized by FLEXCELL use regulated vacuum pressure and positive air pressure to deform flexible-bottomed culture plates. Depending on the type of culture plate, equibiaxial or uniaxial tension may be applied. Flexcell FX-2000 and FX-4000 created by FLEXCELL International Corporation, and recently upgraded to FX-6000 T, were used to promote tensile loading [58–61].

The Flexcell FX-2000 cell-strain unit is composed of a circular silicone rubber membrane at the bottom of each well of the culture plate, in which biaxial strain is regulated by applying vacuum, promoting a multi-radial uniform stretch. One group exposed flexor tendon cells to biaxial tensile strain of 0.0075% at 1 Hz and analysed the formation and organization of the actin stress-fibre network and cell–cell adherent junctions under loading [58]. In another study, the same Flexcell unit was used to apply an equibiaxial cyclic strain of 3% at 0.25 Hz (2 s on, 2 s off) to human mesenchymal stem cells (hMSCs) for 16 days,

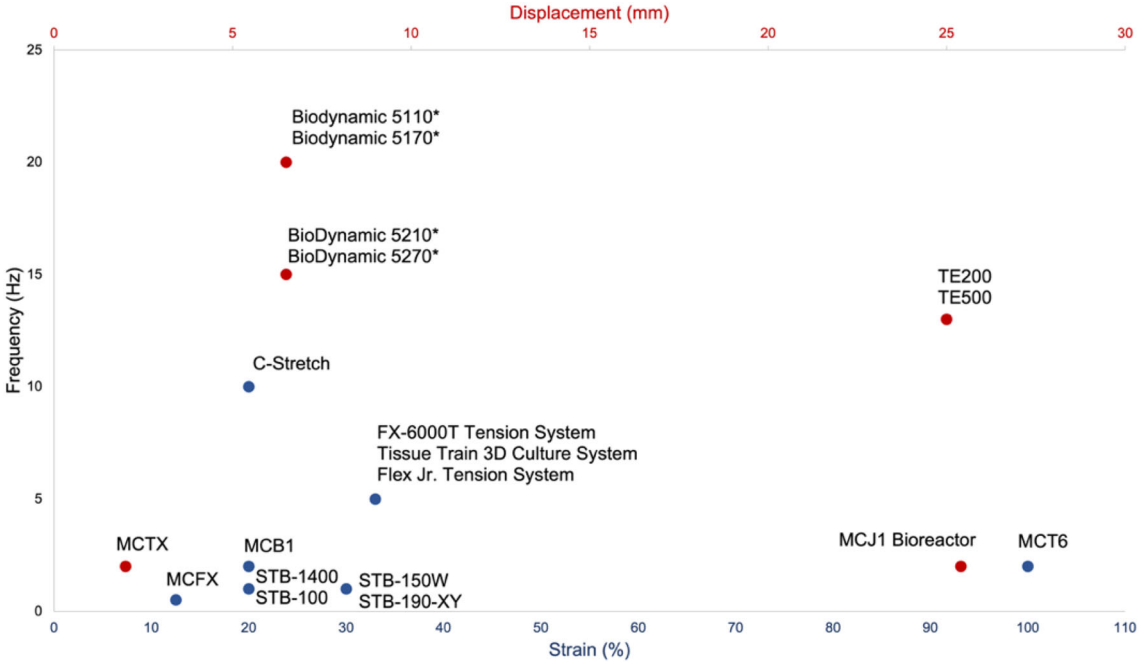


**Fig. 4** Graphical arrangement of the commercially available mechanical stimulation devices according to their maximum strain/displacement and frequency

which decreased proliferation and stimulated matrix mineralization over unstrained cells (Figs. 5a–5c) [59]. Human embryonic stem cells (hESCs) were cultured on BioFlex culture plates coated with Matrigel and exposed to a biaxial 10% membrane strain for 10 cycles/min using the FX-4000 device [61]. The mechanical strain inhibited hESC differentiation, but self-renewal was promoted compared to an unstrained control [61]. Porcine valve interstitial cells and bone-marrow-derived hMSCs (bm-hMSCs) were cultured on BioFlex culture plates and exposed to a biaxial (radial and circumferential) tensile strain of 7%, 10%, 14%, and 20% respectively at 0.6 Hz for 4 days [62]. The strain magnitudes, which were homogenously distributed throughout the membrane, had an impact on collagen production [62]. More recently, the FX-6000 T Tension System was used on vascular smooth muscle cells derived from human-induced pluripotent stem cells (hiPSCs-VSMCs) [63]. Uniaxial cyclic tensile strain of 2.5% at 2.75 Hz applied for a period of 48 h enhanced the expression of VSMC and ECM markers and also the formation of phalloidin, mostly in a perpendicular direction to the tensile loading direction [63]. A Flexcell FX-4000 strain unit was used by Sumanasinghe et al. to apply an uniaxial cyclic tensile strain to bm-hMSCs seeded on linear 3D type I collagen matrices [60]. Cyclic tensile strains of 10% and 12% at 1 Hz induced osteogenic differentiation compared to unstrained controls after 1 and 2 weeks, without osteogenic supplements [60].

Commercialized by IonOptix, C-Pace EM is a multi-mode electromechanical stimulator which can be coupled to the C-Stretch system. This stimulator was used to apply electrical, mechanical, and combined electromechanical stimulation to human-induced pluripotent stem-cell-derived cardiomyocytes (hiPSC-CMs) cultured on fibronectin-coated PDMS [64]. A uniaxial cyclic tensile strain of 5% was applied at 1 Hz for 3 or 7 days and, with regard to electromechanical stimulation, cells were also stimulated with an electrical field of 3 V/cm and 4 ms biphasic pulse duration at the end of the mechanical stimulus hold phase to mimic the isovolumetric contraction. All three stimulus modes resulted in stress-fibre formation and sarcomeric length shortening, but upon electromechanical stimulus the transmembrane calcium current significantly decreased (Figs. 5d and 5e) [64].

A BioDynamic™ chamber mounted on an ELF3200 mechanical testing machine from the TA Instruments group was used in compressive loading studies [65, 66]. Five per cent global strain was applied by cyclic compressive loading (for 2 h on day 9 and then every 5 days up to and including day 19) to hMSCs cultured in 3D polyurethane (PU) scaffolds, and was found to promote osteogenic differentiation and mineralized matrix production [65]. MLO-A5 osteoblastic cells cultured on PU open-cell foam scaffolds were exposed to a compressive strain of 5% at 1 Hz (for 2 h per day on days 5, 10, and 15 of culture), which promoted the production of mineralized matrix (Figs. 5f–5h) [66]. Endothelial progenitor cells (EPCs) isolated from rat bone-marrow were seeded in demineralized bone matrix (DBM) scaffolds under cyclic

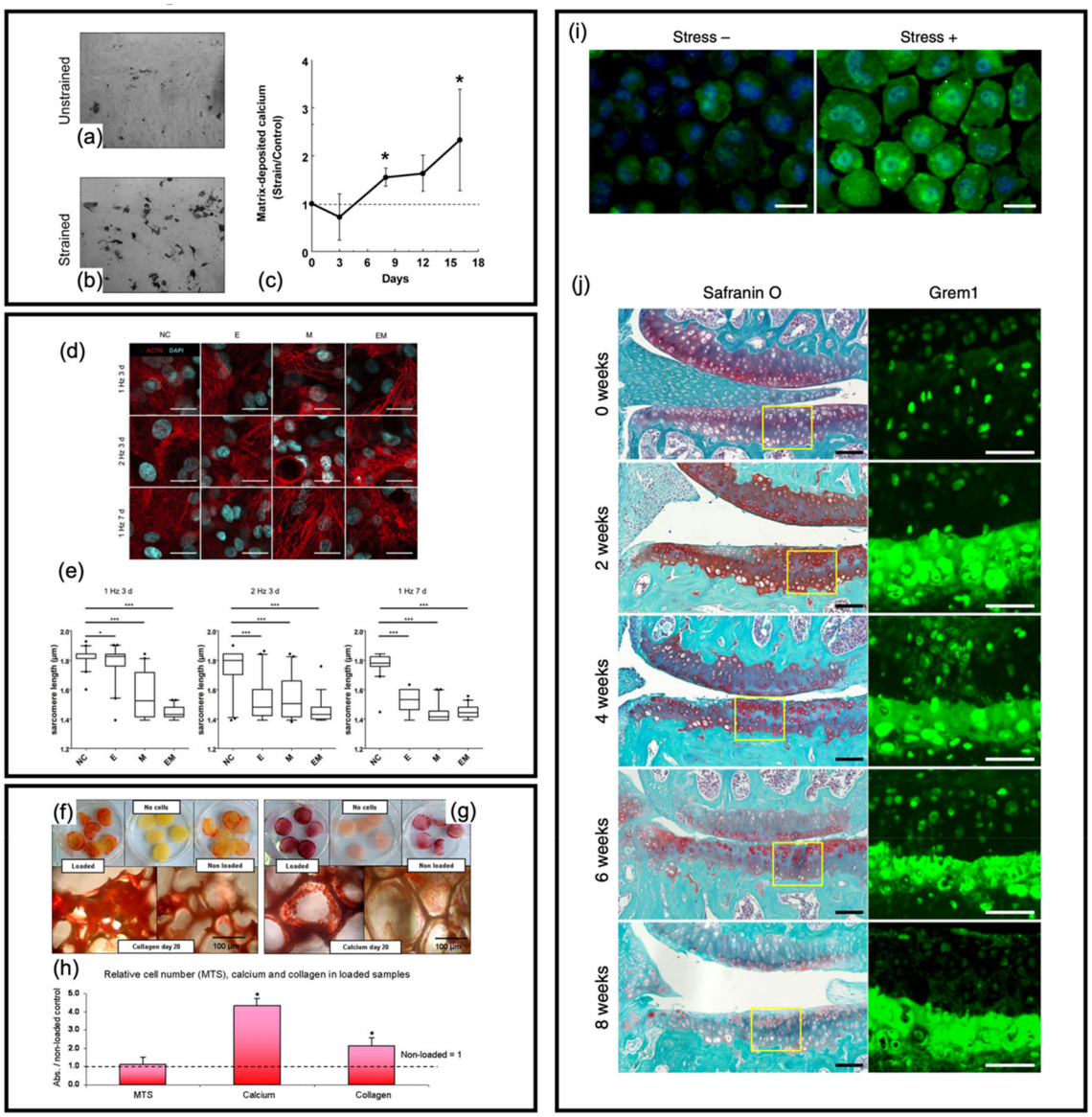


**Fig. 5** Cellular results of studies which made use of commercially available devices. Von Kossa staining of cell layers after 16 days in culture showed that compared to the unstrained condition (**a**), hMSCs that underwent mechanical strain imposed by Flexcell FX-2000 had greater matrix mineralization (**b**), as corroborated by measurement of matrix-deposited calcium (**c**) (reproduced from [59], Copyright 2003, with permission from Elsevier). **d** Sarcomere length analysis by actin (ACTN, red) and nuclei (DAPI, cyan) staining of samples: non-conditioned (NC), electrically conditioned (E), mechanically conditioned by an IonOptix C-stretch (M), and electromechanically conditioned (EM) (scale bar: 25 mm). Results for different conditioning procedures (1 Hz 3 d, 2 Hz 3 d, and 1 Hz 7 d) are shown in a boxplot (**e**) (reproduced from [64], Copyright 2017, with permission from Elsevier). Empty and non-loaded scaffolds were loaded by a TA Instruments BioDynamic device coupled with an Electroforce testing machine, then cut into cross sections and stained with Sirius red (for collagen) (**f**) and alizarin red (for calcium) (**g**). Absorbance of MTS (for cell-viability assessment), alizarin red, and Sirius red per loaded scaffold at day 20 was normalized to a paired non-loaded scaffold (mean±SD) (**h**), and showed an increase of matrix mineralization after loading (reproduced from [66], Copyright 2009, with permission from Elsevier). **i** Expression of gremlin-1 (Grem1) protein (green) in mouse primary chondrocytes increased 24 h after tensile stress loading (stress+) was applied with the Strex STB-140 system, compared to the unloading condition (stress−) (scale bar: 50 μm). **j** An acceleration of mouse osteoarthritis development after surgical induction was observed through safranin O staining and gremlin-1 immunofluorescence. Scale bars: 100 μm and 50 μm, respectively (reproduced from [69] authored by Chang et al. under the Creative Commons license CC BY 4.0). hMSCs: human mesenchymal stem cells

**Table 2** Summary of commercially available devices which apply tensile and/or compressive stresses

| Company | Product model | Stress type | Loading capacity | Maximum strain (%) or displacement (mm) | Maximum frequency (Hz) |
|---|---|---|---|---|---|
| FLEXCELL International Corporation | FX-6000 T Tension System | Uniaxial/biaxial tensile stress | | 33% | 5 |
| | FX-5000C Compression System | Uniaxial compressive stress | 62 N | | |
| TA Instruments | Biodynamic 5110* | Uniaxial tensile/compressive stress | 200 N | 6.5 mm | 20 |
| | Biodynamic 5170* | Uniaxial tensile stress | | | |
| | BioDynamic 5210* | Uniaxial tensile/compressive stress | | | 15 |
| | BioDynamic 5270* | Uniaxial tensile stress | | | |
| CellScale | MCB1 | Biaxial tensile stress | 10 N | 20% | 2 |
| | MCFX | Uniaxial tensile stress | 30 N | 12.5% | 0.5 |
| | MCT6 | | 200 N | >100% | 2 |
| | MCTR | Uniaxial compressive stress | 700 kPa | | 0.5 |
| | MCTX | | 100 N | 2 mm | 2 |
| | MCJ1 Bioreactor | Uniaxial tensile stress | 100 N | 25.4 mm | 2 |
| IonOptix | C-Stretch | Uniaxial tensile stress | | 20% | 10 |
| BISS | TE200 | Uniaxial tensile/compressive stress | 200 N | 25 mm | 13 |
| | TE500 | | 500 N | | |
| | TE40[a)] | | 40 N | 4.5 mm | |
| Strex | STB-1400 | Uniaxial tensile stress | | 20% | 1 |
| | STB-100 | | | | |
| | STB-150 W | | | 30% | |
| | STB-190-XY | Biaxial tensile/compressive stress | | | |

[a)]The device also allows a pulsatile flow stimulation

compressive loading. Cell-based constructs were placed in a BioDynamic ELF5110 device, and after being subjected to 5% strain at 1 Hz for 4 h/day for 7 days, proliferation of EPCs increased [67].

Cell tensile loading systems from Strex are reported in the literature for diverse purposes, including the evaluation of cell adhesion and mechanotransduction studies. Meniscal root and horn cells were cultured on rat tail COL1-coated polydimethylsiloxane and subjected to 2 h and 4 h treatment with 5% and 10% uniaxial cyclic tensile strain at 0.5 Hz, using a STB-140 system. The density of both root and horn cells was reduced after mechanical treatment, whereas expression of the chondrocyte-associated genes SOX9 and COL2A1 was significantly enhanced [68]. Using the same loading system, mouse primary chondrocytes were seeded into silicon stretch chambers coated with fibronectin, and after 48 h were subjected to cyclic tensile loading (0.5 Hz, 10% elongation) for 30 min in a $CO_2$ incubator. The excessive loading accelerated osteoarthritis development by inducing gremlin-1 (Figs. 5i and 5j) [69]. In a different study, Murali et al. seeded hMSCs onto silicone chambers coated with COL1 and subjected them to tensile loading at 1 Hz frequency and 8% strain for 6, 24, 48, and 72 h, using the ST-140 model. They suggested that when subjected to uniaxial loading, hMSCs underwent tenogenic differentiation through activation of epithelial sodium channels [70]. Takahashi et al. seeded normal human lung fibroblasts onto silicon chambers coated with COL1, and a uniaxial sinusoidal cyclic tensile loading of 30 cycles/min was applied for 10 min using the ST-140 model. The concentrations of ATP in the supernatant were significantly elevated by 20% strain, but not by 4% strain. The researchers also visualized ATP release during

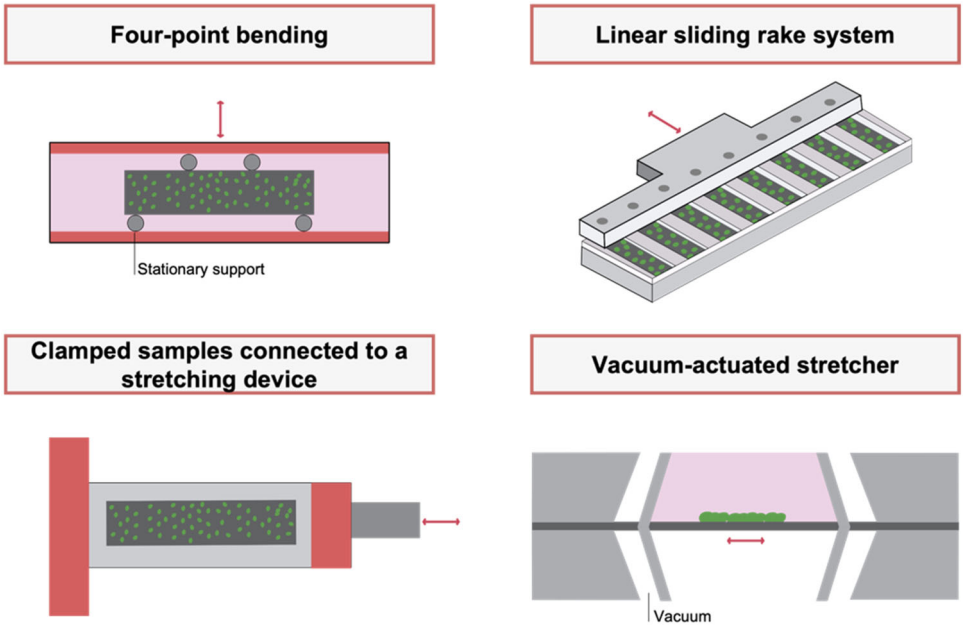


**Fig. 6** Representation of four tensile working principles. In the four-point bending apparatus, the cell-based construct is supported by stationary supports and strain is distributed in the perpendicular plane to the applied load. However, the strain magnitude is not distributed uniformly between these horizontal planes because it increases from the central horizontal axis to the external medial and lateral faces (which are subjected to maximum tensile and compressive strains, respectively) [73]. Constructs can also be placed in cages and fixed at two opposite ends: one rigidly and the other to the rake attachment. The linear sliding rake is then controlled at the desired frequency and amplitude. Cell-based samples can also be clamped and connected to a tensile device (one end of the rectangular membrane is fixed while the other is connected to a computer-controlled movable frame). Finally, polymeric substrates may be exposed to uniaxial tensile loading with a vacuum-actuated tensile device. The movement imposed by the tensile loading device is represented by the red arrow

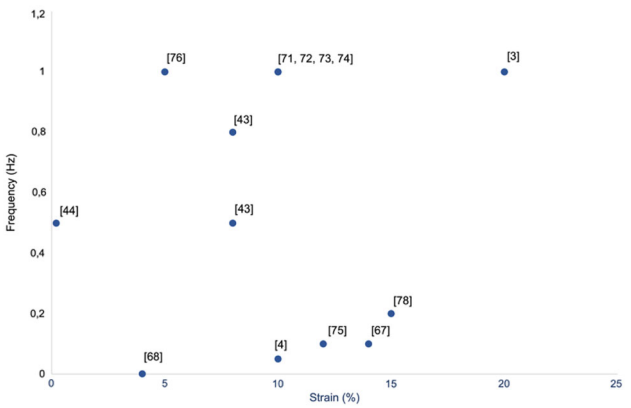


**Fig. 7** Graphical arrangement of the devices designed and produced by research groups according to the maximum tensile strain/displacement studied at a particular frequency. Observation: despite the fact that Subramanian et al. [57] applied 2% uniaxial tensile strain to cells encapsulated in collagen constructs, the device used in this study may operate at a loading strain up to 12% at cyclic frequencies of 0.01–1 Hz

cell stretch in real time, using the NS-600 W model. Following a single uniaxial tensile strain of 22% for 1 s duration, the release of ATP continued and increased in intensity [71].

Besides application of tensile or compressive stresses, all models of TA Instruments presented in Table 2 include pulsatile stimulation. For example, the BioDynamic 5170 and BioDynamic 5270 test instruments permit a flow range of 17–1760 mL/min. These devices are computer-controlled, allowing a static, cyclic, or intermittent deformation in a range of frequencies, amplitudes, and waveforms. The substrates used for culture plates of commercialized mechanical stimulation devices are typically flexible and light-transparent materials that enable phase-contrast, fluorescence, or scanning confocal microscopy analysis. The design and material choices allow, in some cases, simultaneous and real-time visualization using inverted microscopes. While these are often preferred to upright microscopes because they do not limit the total height of the device, it is mandatory to ensure that the focal length is not compromised. Despite the notorious progress on the tensile and compressive loading devices available on the market, the main motivation for research groups to design and fabricate their own devices is related to these device-associated costs. The cost of these devices ranges from thousands to tens of thousands of dollars, and the total price may increase when considering maintenance and the need to purchase additional device-specific

**Table 3** Loading features of the uniaxial tensile loading applied by the custom-built devices to the cell-based constructs, grouped by the device working principle

| Device working principle | Loading capacity | Maximum strain (%) or displacement (mm) | Frequency | Experiment duration | Cell-based construct | Ref. |
|---|---|---|---|---|---|---|
| Four-point bending apparatuses | 2 N | 0.2 mm | 5 mm/min | 250 cycles every 24 h for 16 days | Human bm-MSCs on DMB scaffolds | [74] |
| | | 0.2% | 0.5 Hz | 40 min at 0, 0.5, 1, 2, 6, 12, and 24 h | Rat bm-MSCs on flexible silicon-bottomed chambers | [43] |
| Linear sliding rake system | | 0%–10% | 1 Hz | 48 h and for 68 h | Bovine articular chondrocytes and MFC seeded on fibrin hydrogels | [53] |
| | | 10% | 1 Hz | Short (24 h) or extended (1–2 weeks) periods | Calf bm-SC-seeded fibrin hydrogels | [54] |
| | | 10% | 1 Hz | 3 h followed by 3 h without loading for 21 days | Human bm-SCs encapsulated on PEG-based OPF hydrogel | [55] |
| | | 10% | 1 Hz | 10–120 min and for 10 min every 6 h for up to 6 days | Human bm-MSCs cultured in collagen-CG scaffold | [56] |
| | 1–3 N | 2% | 0.1 Hz | 1 h/day for 3 days | Human cardiomyocytes AC10, murine myoblasts C2C12, and murine osteoblasts OB6 encapsulated in collagen constructs | [57] |
| Clamped samples connected to a tensile device | | 5% | 1 Hz | 4 h for 2 days | Wistar rat MSCs cultured in porous CG scaffold | [75] |
| | 2.5 N | 4% grip–grip | 0.001 Hz | 30 min/day for 3 days | Mouse-derived MSCs seeded on PEUUR coated with fibronectin | [51] |
| | | 2% and 8% | | Three times 2 h/day for 3 days | Human bm-MSCs on elastic silicone | [76] |
| | 9.81 N | 10% | 0.05 Hz | 720 cycles/day for 3 days | Murine MSCs encapsulated in collagen type I sponges | [4] |
| | | 10% | 1 Hz | 18 h | Mouse bone-marrow-derived macrophages cultured on fibronectin-coated silicone | [3] |
| | | 20% | 1 Hz | From 0.5–1 h after seeding to 6.5–7 h after seeding | Neonatal rat ventricular myocytes cultured on fibronectin-coated silicone | |
| Vacuum-actuated tensile device | | 0%, 3%, 7% and 14% | 0.1 Hz | 2 days under loading, 2 days under static and then 2 days under loading | NIH3T3 cultured on PDMS | [52] |
| | | 1.5%, 3%, 8% | 0.5 Hz | 1, 2, and 7 min (respectively) | hiPSC-CMs cultured on PDMS | [42] |
| | | 8% | 0.8 Hz | 2, 4, or 7 days | | |
| | | 5%–15% | 0.2 Hz | 5 h and 5 days (short and long-term, respectively) | Human alveolar epithelial cells and human pulmonary microvascular endothelial cells cultured on opposite sides of the PDMS membrane | [77] |

Substrate: demineralized bone (DMB); oligo(poly(ethylene glycol) fumarate) (OPF); poly(ethylene glycol) (PEG); collagen-glycosaminoglycan (CG); poly(esterurethane urea) (PEUUR). Cells: meniscal fibrochondrocytes (MFC); stromal cells (SC); human-induced pluripotent stem cells-derived cardiomyocytes (hiPSC)

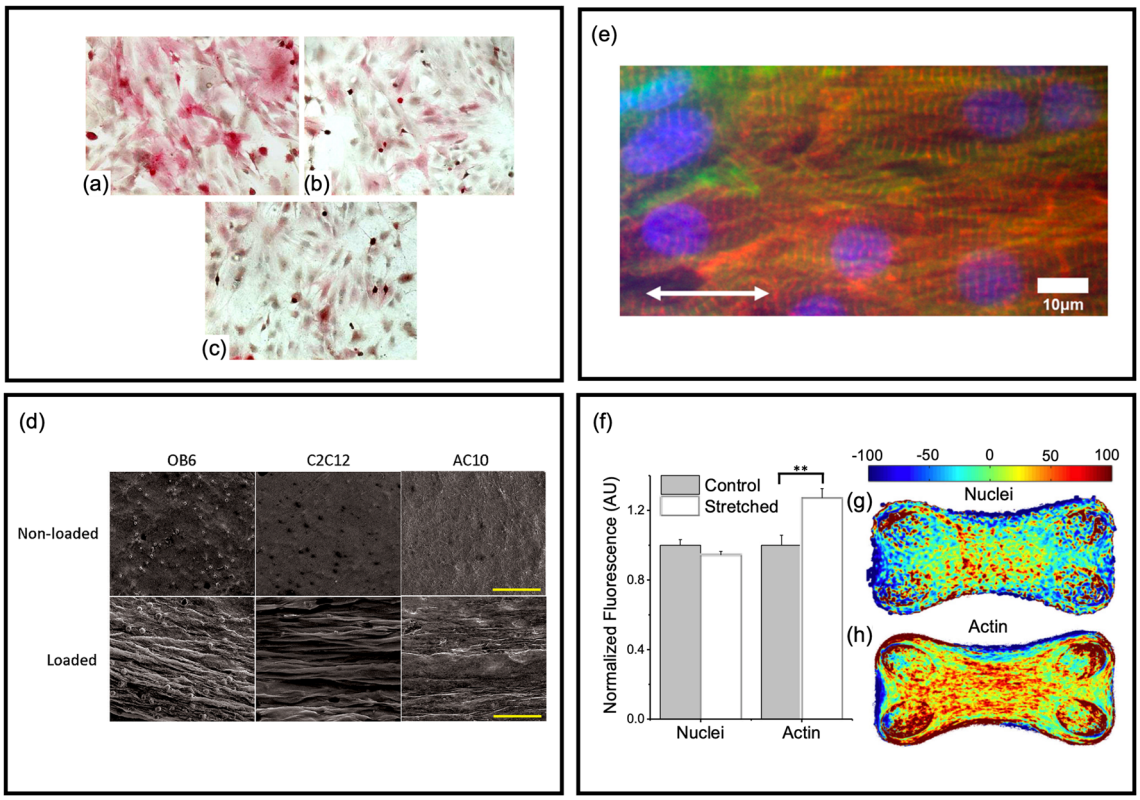


**Fig. 8** Results of studies performed with customized tensile loading devices. ALP staining at 24 h was higher for cells subjected to mechanical loading by a four-point bending device (**a**) compared to unstretched cells (**b**) and control cells (**c**) (reproduced from [43], Copyright 2008, with permission from Elsevier). **d** Scanning electron micrographs of 3D collagen constructs encapsulated with OB6, C2C12, or AC10 cells at day 3 either loaded by a linear sliding rake system or non-loaded (scale bar: 100 μm) indicated that the fibre orientation of loaded cells was parallel to the axis of load application (reproduced from [57], Copyright 2017, with permission from Wiley). **e** Staining of actin (green), sarcomeric z-lines (red), and nuclei (blue) of cardiomyocytes cultured on clamped samples connected to a tensile device revealed that after being subjected to 6 h of cyclic uniaxial tensile loading, the cells aligned in the direction of loading (white arrow) (reproduced from [3], Copyright 2018, with permission from ASME). **f** No significant differences in the average normalized total fluorescence of nuclei were found between non-stretched (control) and stretched groups, but F-actin fluorescence significantly increased with loading performed with a vacuum-actuated tensile device. The spatial distribution of per cent change between stretched and control average nuclei (**g**) and F-actin fluorescence (**h**) showed that expression of F-actin increased after tensile loading (reproduced from [52], Copyright 2018, with permission from Springer Science Business Media, LLC, part of Springer Nature)

accessories (such as culture well plates) in order to maximize the number of samples that can be tested at the same time [3]. Moreover, the macroscopic dimensions of some devices limit their throughput, and it is usually difficult or impossible to adapt to particular experiments such as, for example, using other substrate materials than polymers, which restricts the utility of these devices in a research context [3, 51, 52, 72].

## Custom-built cell-stimulation devices

Despite the focus on continuous innovation, mechanical stimulation systems available on the market present critical challenges. Consequently, numerous research groups have designed and developed custom-built devices to study the effects of tensile and compressive loading conditions on cellular behaviour.

### Tensile loading devices

Several tensile loading devices with different designs and working principles have been developed in recent years. Table 3 lists uniaxial tensile loading studies in which devices were custom fabricated to meet research groups' needs. The tensile loading working principles were divided into four major groups: four-point bending apparatuses, linear sliding rake systems, clamped samples connected to a tensile device, and vacuum-actuated tensile devices, as represented in Fig. 6. The tensile loading devices designed by research groups are graphically arranged in Fig. 7, according to the maximum strain/displacement and frequency under study.

The majority of tensile loading devices involve cell culture on a circular flexible membrane (fixed along its periphery) or rectangular flexible membrane (fixed at opposite ends)

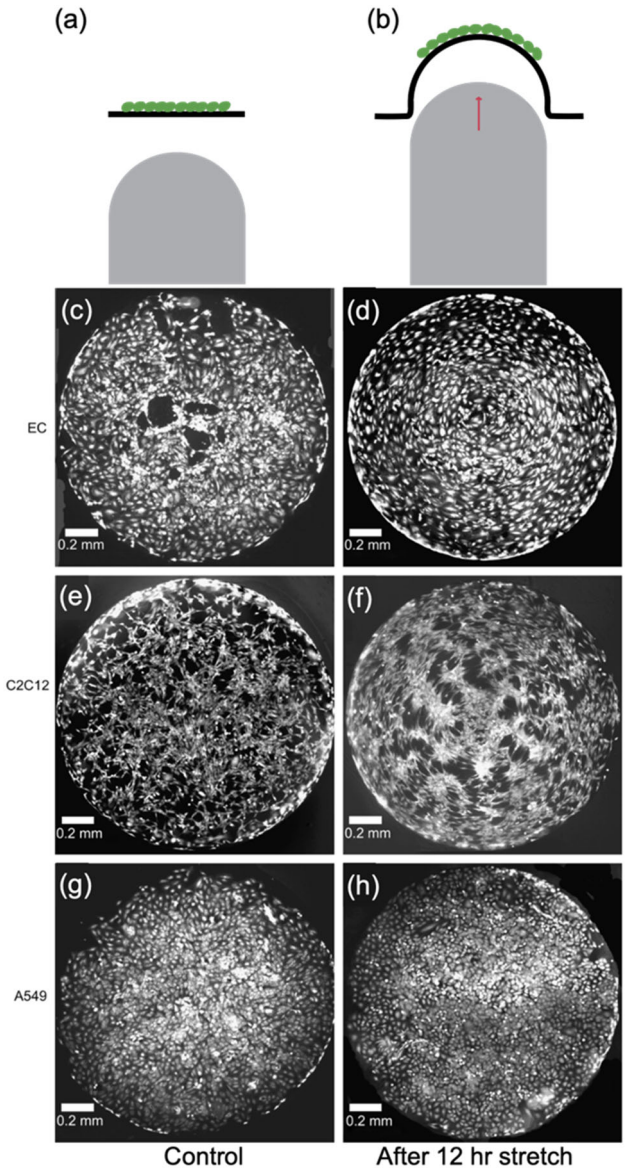


**Fig. 9** Schematic representation of the cross section of cells (represented in green) cultured on flexible membranes (**a**) and the deformation of the latter as the pin moves upwards (**b**). The alignment of C2C12 and HDMECs in response to loading is illustrated by fluorescent images of HDMECs (**c**, **d**), C2C12 myoblast cells (**e**, **f**), and A549 alveolar epithelial cells (**g**, **h**) stained with Calcein AM before loading (left column) and after being subjected to cyclical tensile loading (5 Hz for 12 h) (right column) (reproduced from [72], Copyright 2008, with permission from Elsevier). HDMECs: human dermal microvascular endothelial cells

(Fig. 7). Some of the results obtained by the studies mentioned in Table 3 are summarized in Fig. 8.

Application of cyclic uniaxial (one direction) tensile strains sometimes leads to a heterogeneous biaxial strain profile, due to the Poisson effect. Therefore, custom-designed devices were developed to modulate equiaxial strains and generate a homogeneous strain environment [32, 44, 78, 79]. Other groups focused on reproducing a more complex physiological environment by applying biaxial strains [80, 81]. Tensile loading was also performed using piezoelectrically actuated pins of a Braille display [72]. Briefly, an elastomeric membrane of PDMS containing microwells was placed on top of an actuated pins array and deformed by the Braille pin movement. Each pin was independently computer-controlled and responsible for applying a cyclically radial strain (maximal 20%–25% radial and 12% tangential). Mouse myogenic C2C12 cells and human dermal microvascular endothelial cells (HDMECs) aligned to the loading direction at increasing frequencies of 0.2, 1, and 5 Hz, after 2, 4, and 12 h, in contrast to human lung adenocarcinoma epithelial A549 cells, which did not respond to tensile loading (Fig. 9) [72].

### Compressive loading devices

Microfabricated devices have been developed to apply compressive strain to cell-encapsulated constructs. Typically, the compression is achieved by loading pistons actuated by a pneumatic system. This type of compressive device can generate three types of compression: unconfined, semi-confined, and confined, all of which are illustrated in Fig. 10.

Unconfined compression was studied in the majority of compressive loading studies, as it represents the simplest microfabrication technique. One device was designed to study the influence of dynamic 10% compressive strain at 1 Hz for up to 3 weeks on chondrogenesis of goat bm-MSCs encapsulated in poly(ethylene glycol) diacrylate (PEGDA) hydrogels, as well as human embryonic body-derived (hEBd) cells encapsulated in tyrosine-glycine-aspartate-serine (YRGDS)-PEG-acrylate hydrogels [82]. The expression and synthesis of chondrocyte-specific matrix molecules were also studied, under the same loading conditions, with bovine bm-stromal cells encapsulated in agarose gels for 8 and 16 days [83]. Another group investigated the role of cyclical unconfined compression on osteogenesis by applying 10% and 20% compressive strains at 0.5 Hz for 4 h on rat pre-osteoblasts seeded into electrospun polycaprolactone (PCL) scaffolds [84]. Only the 10%-magnitude strain induced expression of osteogenic-related proteins and transcription factors, showing that elevated magnitudes may inhibit bone formation [84]. Ravichandran et al. designed a custom-fabricated device to apply a range of compressive strains to four independent chambers. hMSCs were seeded on polycaprolactone-β tricalcium phosphate (PCL-TCP) scaffolds using fibrin gel and then exposed to 0.22%, 0.88%, and 1.1% compressive strain at 1 Hz, 4 h/day for 4 weeks [85]. Cyclic physiological compression of 0.22% resulted in higher ALP activity compared to supra-physiological strains; it also up-regulated osteogenic markers and generated high mineralization levels [85]. C3H10T1/2 mouse MSCs were encapsulated in PEG hydrogels and exposed to 6%, 11%,

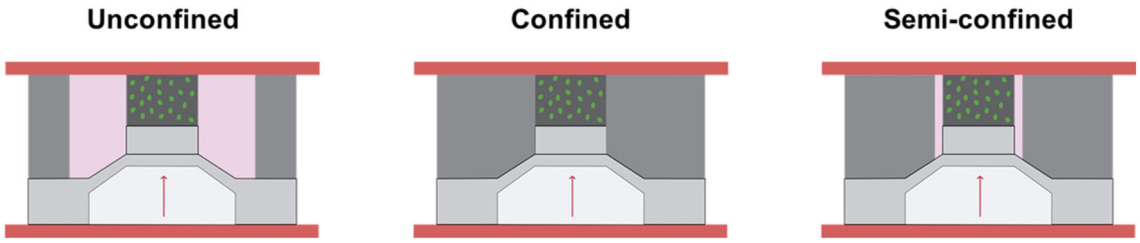


**Fig. 10** Illustration of compression models: unconfined compression, confined compression, and semi-confined compression. The three-dimensional cell-based construct is compressed by the movement of a piston, in this case as a result of pressurized air (represented by the red arrow)

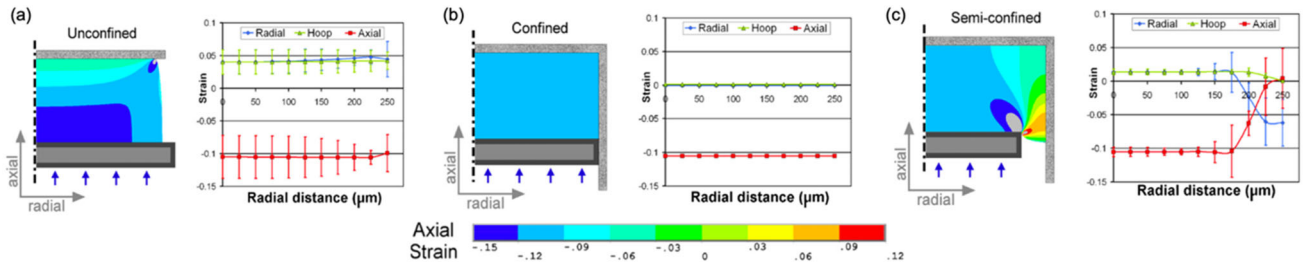


**Fig. 11** Finite-element simulations of three compression modes all involved application of 10% compressive strain on PEG hydrogel (adapted from [88], Copyright 2011, with permission from IOP Publishing Ltd). Strain field within the hydrogel was generated for unconfined (**a**), confined (**b**), and semi-confined (**c**) compression modes and the radial, circumferential, and axial strains (mean and standard deviation) were plotted for the total axial thickness of the hydrogel

14%, and 26% compressive strains. Regardless of the strain magnitude, there was no significant difference in nuclear deformation, whereas cellular deformation only changed significantly at the highest strain levels [86]. The device proposed by Moraes et al. [86] consisted on an array of loading posts suspended over actuation cavities and was adopted and altered by Lee et al. to subject alginate-chondrocyte constructs to compressive strain [87]. These constructs were placed on PDMS balloons with different diameters and by varying only the cavity diameter (with the applied pressure remaining the same), it was possible to create a range of compressive strains. Because the balloons were inflated with pressurized air, compression on constructs was studied either in a static (14 kPa, 1 h) or dynamic (14 kPa, 1 Hz, 1 h) mode. Lee et al. found that the mean strain of chondrocytes was approximately 50% of the gel strain, with a permanent deformation of 9%–30% for static compression, and 0.5%–6% for dynamic compression. Finally, cell viability was found to be higher in dynamically loaded constructs, perhaps due to better nutrient transport [87]. Despite these findings, unconfined compression generates a heterogeneous strain distribution within the 3D construct. In contrast, confined compression generates a uniform strain, but challenges arise concerning its microfabrication. Semi-confined compression offers easier microfabrication, but uniform strains are only achieved in the central region of the biomaterial. These findings were obtained from the finite-element simulations (represented in Fig. 11), and the obtained strain fields for the three compression modes were compared [88].

The same group fabricated a semi-confined compression device, which was used to generate nominal strains of 20%, 30%, 40%, and 45% on PEG and collagen hydrogels. The authors concluded that this compression model enables the study of cellular responses to precisely applied strains on a range of polymerizable biomaterials, improving the applicability and versatility of the device [88]. Zhang et al. [89] used a custom-designed dynamic-compression loading system with a stepper motor to apply a 10% compressive strain on PCL scaffolds encapsulated with hMSCs. PCL-based constructs subjected to both mechanical and biochemical stimulation supported a chondroprotective effect [89].

## Review of patents

Given the promising outcomes from engineered mechanical stimulation devices in mechanobiology studies like those described above, many patent applications have been filed in the past few decades. We looked at both granted patents and patent applications, and conducted our research through the Derwent Innovation Index [90] and Google Patents [91] databases, which include European, USA, and World Patents (WIPO—World Intellectual Property Organization). The keywords were related to mechanical cell stimulation and resulted in a total of 369 records. We excluded inventions

whose descriptions could not be automatically translated to English, those with unclear abstracts, and those not within the scope of this review.

A total of 44 patents of devices able to create different stimuli (tensile, compressive, shear stresses, and vibration) were comprehensively studied and selected, taking into account their in vitro cellular purposes. Table 4 summarizes the selected inventions. They are organized first by frequency level (low to moderate vs. high frequency), then by actuator type, as schematically illustrated in Fig. 12, and finally by the imposed stress state. Inventions that obey non-conventional actuation principles are in a separate category.

To better organize the resulting inventions, we grouped them according to their actuation principle. From low to high frequencies, the actuation may be pneumatic (either positive or negative pressure), motor-driven, or magnetic. However, some inventors disclosed more than one functionality principle. The invention of Sittampalam et al. [96] is a drug-screening device and system that attempts to impart strain to cells in a similar manner to physiological motion and rest. According to their description, different mechanical drive systems can be adopted to move the pins and thus exert mechanical strain on cells, including a linear actuator (Fig. 13a), an electromagnetic system, or a pneumatic system (Fig. 13b).

The device invented by Shapiro et al. [118], defined in Table 3 as belonging to the motor-driven category has, in fact, more than one approach to achieving membrane mechanical displacement (Fig. 14). The elastic membrane upon which the cell culture is placed is securely held in place and moved by a displacement applicator located, for example, on the bottom surface. Then, it is cyclically moved upward and downward by a force generator, deforming the membrane. This membrane deformation imparts biaxial forces (either tensile or compressive) to the cells mounted thereon, and the strain profile may be either uniform or non-uniform. The electric motor drives an actuating apparatus, such as a cam (Fig. 14a), which revolves eccentrically about an axis, contacting the bottom surface of the rod and forcing the rod and displacement applicator to move upward to contact and deform the membrane. At the end of the upward stroke, the applicator moves to a lowered position out of contact with the membrane. The invention may also correspond to a mechanical actuated tensile apparatus which applies biaxial strain (Fig. 14b) or simultaneously applies tensile loading to several cell cultures (Fig. 14c). The removable and disposable wells are mounted above each available displacement applicator.

Substrate deformation through the pneumatic actuation principle may be achieved by pressure [92, 98] or vacuum [93–97], and by pulling a portion of the flexible membrane upward or downward, respectively. Despite the simple set-up, in both modes the stimulus frequency is low and may not even be capable of creating dynamic cycles. However, vacuum pumps are slower than pressure inlet. Other inventions aim to deform the membrane through pressurization of the fluid (e.g., culture medium) [99, 102], or by creating hydrostatic pressure using a piston [100]. If not carefully designed, moving the flexible membrane upward through a displacement applicator, by pressure or manually (e.g. with a piston), may cause friction between the membrane of interest and the loading post of the device, as represented in Fig. 15.

Hydraulic actuators are comprised of a hollow cylinder with a piston, and due to unbalanced pressure applied to the piston, a force is generated that deforms the membrane equiaxially. Although these actuators are often limited in terms of frequency, invention number DE102009057698A1 of Kiesow et al. [98] allows cyclic testing in a frequency range of 0.001 to 200 Hz.

Still, either in low- or high-frequency mode, the culture liquid in contact with the cells may be pressurized and the generated hydrostatic pressure then exerts a compressive mechanical force on cells.

The motor-driven mechanism involves the conversion of a rotary motion of an electric motor into linear displacement. The selected motor may be a stepper motor [103, 104, 106–111, 117], a linear DC motor [105, 113, 114, 119, 128], a servo motor [126], or a voice-coil motor [105, 115]. Stepper motors, which are composed of multiple toothed electromagnets, were preferred for some of these inventions. Despite the possibility of miniaturization, precise rotation (ranging from step angles through full 360° rotation), easy set-up and control, this type of motor is frequently slow due to a low transmission ratio (from rotational to linear movement). Moreover, it may cause small vibrations, which will act as an external disturbance to the system and thus should be considered separately from the substrate's deformation. Linear DC motors are two-wire continuous rotation motors with each pulse being so fast that the motor seems to be rotating constantly with no stuttering. Servo motors are also fast, with high torque, and can be precisely controlled because of their accurate rotation within a limited angle. This actuation principle is particularly suitable for uniaxial tensile loading and for larger engineered constructs. In addition, it allows multiple loading modes and precise control over the strain features, such as amplitude and frequency. On the other hand, some potential disadvantages are the risk of contamination and limitation of high-throughput capabilities [134].

The linear actuation principle may be preferable because it allows for automation, requires less maintenance, and offers a broader range of strain magnitudes, frequencies, and durations of mechanical stimulus. Invention number US10,421,955B2, assigned to IonOptix LLC in 2019 (Fig. 16), applies a tensile strain up to 50% (at 0.01–10 Hz) on a deformable rectangular culture dish made, for example, from silicone rubber [111]. A plurality of viewing ports are

**Table 4** Overview of inventions related to mechanical stimulation of cells

| Frequency | Actuator type | | Stress state | Patent number | Publication year | Description | Observation | Ref. |
|---|---|---|---|---|---|---|---|---|
| Low to high | Pneumatic | Pressure | Radial/equiaxial | WO 2,009,039,640 A9 | 2009 | A positive pressure is delivered to several actuation devices, generating tensile strains in the range of 0%–200% | Each actuation device can also be connected to vacuum to apply compressive strains in the range of 0%–80% | [92] |
| | | Vacuum | | US 4,839,280 | 1989 | Individual vacuum ports are affixed beneath each well base and the elongation of the membrane can be constant or cyclic, or may be irregular or applied in a pattern, as desired | The flow means disposed between the plenum and vacuum source is a solenoid valve electrically connected to a computer | [93] |
| | | | | US 10,246,676 B2 | 2019 | Vacuum pressure is applied to the cell-containment part, the bottom surface of which is made of flexible polymer material | | [94] |
| | | | Equibiaxial, uniaxial, or other stretching direction | US 6,472,202 Bl | 2002 | A central opening defined in the planar member allows a vacuum to be drawn through and to pull a portion of the flexible membrane downward | | [95] |
| | | | Equiaxial | US 2013/0059324Al | 2013 | Below the flexible membrane is a pin plate (one pin per well) that applies compressive or tensile loading to the membrane bottom | The mechanism to actuate the pins can include a mechanical linear actuator (e.g. a non-circular shaft coupled to a movable support) or electromagnetic system | [96] |

**Table 4** (continued)

| Frequency | Actuator type | Stress state | Patent number | Publication year | Description | Observation | Ref. |
|---|---|---|---|---|---|---|---|
| | | | US 2015/0050722A1 | 2015 | The cell culture plate is operatively coupled to a plenum device | The device may also deliver electrical stimulation | [97] |
| | Hydraulic pressure | Equiaxial | DE102009057698A1 | 2011 | A porous carrier membrane with an elastic breaking strain of 20%–100% separates two reactor part volumes (one filled with liquid cell culture and the other with gas atmosphere) | The support membrane is deformable through a pneumatic and/or hydraulic control device and volume, which is implemented as two magnet valves and/or as a reciprocating piston. Frequency in the range of 0.001 to 200 Hz | [98] |
| | Hydrostatic pressure | | US 8,980,624 B2 | 2015 | A fluid pressure device supplies a pressurized fluid to the pressure chamber to deform the membrane and move the pressurizing member downward in each culture chamber, thereby exerting a mechanical compression force on cells | | [99] |
| | | | US 9,303,244 Bl | 2016 | A piston moving in and out of a cylinder generates pressures at high physiological levels up to at least 10 MPa | The device may be configured to generate negative pressure or vacuum, wherein the chamber further includes a bleeding passageway for passing air or the gas | [100] |

**Table 4** (continued)

| Frequency | Actuator type | Stress state | Patent number | Publication year | Description | Observation | Ref. |
|---|---|---|---|---|---|---|---|
| | | | US 2020/0339936 Al | 2020 | A magnetic component drives the moving component to shift between a non-pressurizing and a pressurizing position, and the moving component moves towards the bottom chamber surface and pressurizes the cell sample | | [101] |
| | | | WO 2009/047045 A2 | 2009 | Actuating means comprise at least one first piston responsible for pressurization of the culture liquid contained in the sideways chamber, generating compression | The device may also apply constant or cyclic direct compressive and shear stresses upon perfusion and simultaneous hydrostatic pressure and shear stress | [102] |
| | Motor-driven | Uniaxial | CN1834220A | 2006 | A stepper motor is connected to a leading screw and a pressure baffle plate which squeezes the test sample to within the 50–300 mN range | | [103] |

**Table 4** (continued)

| Frequency | Actuator type | Stress state | Patent number | Publication year | Description | Observation | Ref. |
|---|---|---|---|---|---|---|---|
| | | | WO 2017/152080 A1 | 2017 | The mechanical loading system comprises one fixed plate and at least one movable plate, each having several pins for holding at least a portion of the tensile loading chamber. The driving mechanism is configured for moving the movable plate in a uniaxial direction towards and away from the fixed plate | No gripping is required, so there is no risk of disintegration of mechanically fragile scaffolds during the fixation process | [104] |
| | | | WO 2013/090738 A9 | 2013 | A linear actuator bears against the specimen, which may be supported in a Petri dish, generating axial compression | | [105] |
| | | | CN101372664A | 2009 | A motor driven bar is coupled to one extremity of the tissue to be cultivated and used to generate axial tensile and compressive stresses, and rotation | | [106] |
| | | | CN102433258B | 2012 | The cell culture material is fixed on a fixed support and a sliding support is connected to a stepper motor, generating tensile loading | Also establishes electrical stimulation (constant voltage, pulsed voltage, or DC micro-electric stream) | [107] |

**Table 4** (continued)

| Frequency | Actuator type | Stress state | Patent number | Publication year | Description | Observation | Ref. |
|---|---|---|---|---|---|---|---|
| | | | CN103966094A | 2014 | Elongation of the membrane is achieved with a cytoskeleton self-clamping module, in which one end is fixed and the other is moved | | [108] |
| | | | US 2012/0100602 Al | 2012 | A sliding arm applies mechanical displacement in a predetermined direction, generating tensile, compressive, or a hybrid of both stresses | The sliding arm is connected to an actuator that can be powered by a high-precision stepper motor | [109] |
| | | | US 9,617,507<br>US 10,421,955 B2 | 2017<br>2019 | Several culture dishes are mounted to a fixed support and to a movable support by mounting posts, which are connected to a stepper motor coupled to tensile output (frequency: 0.01–10 Hz; Stretch: 0%–50%) | The tensile output can drive one or more solenoids to provide a range of motion for the moving support. It also allows electrical stimulation (frequency: 0.01–99 Hz; Pulse duration: 0.4–24 ms; Voltage: ±40 V and 240 mA) | [110]<br>[111] |
| | | | US20180164278A1 | 2018 | A three-dimensionally designed support structure admits the cell culture and is subjected to tensile or compressive forces by actuators attached to the holding rack | At least one of the actuators and/or counter-actuators is a piezo actuator, an electrothermal or electrically active polymer actuator, or an electromechanical, electrochemical, magneto-strictive, hydraulic, pneumatic, bimetallic, or electromagnetic actuator | [112] |

**Table 4** (continued)

| Frequency | Actuator type | Stress state | Patent number | Publication year | Description | Observation | Ref. |
|---|---|---|---|---|---|---|---|
| | | | WO 2011/013067 A2 | 2011 | Extension and relaxation of the substrate following translation of a rod controlled by a linear electric motor. The deformation and the force applied to the substrate can be controlled based on feedback control signals from the linear motor or from a load cell placed in the culture chamber | It is possible to use an alternative motor or other driving system (these obtain an axial movement of the stem) or a hydraulic or pneumatic actuator (devices in which a piston is controlled by oil, compressed air, or another fluid) | [113] |
| | | | WO 2017/125159 A1 | 2017 | A tensile strain of 5% to 10% is applied to the cell culture (frequency from 0.5 to 1.5 Hz). Two magnets are placed outside the culture plates, one static, to fix one end of the silicone construct, and the other to pull the other end following a programmable pattern, thanks to a computer-controlled linear motor | Electrical pulses may be applied to cells having a potential value from 10 mV/cm to 1000 mV/cm at a frequency between 0.5 and 1.5 Hz | [114] |

**Table 4** (continued)

| Frequency | Actuator type | Stress state | Patent number | Publication year | Description | Observation | Ref. |
|---|---|---|---|---|---|---|---|
| | | | US 2012/0219981 Al | 2012 | Two engagement areas are located at opposite ends of the flexible substrate, and each is connected to a motor, such that either one end or both ends are stretched in opposite directions with respect to each other (up to 100% in its length from 0.5 to 10 Hz) | A voice-coil-based motor may be used in the tensile system instead of a stepper motor to minimize heat generation during operation | [115] |
| | | | CN101649291A | 2009 | Periodic or continuous dynamic tensile or compressive loading can be applied to a plurality of cell culture units simultaneously with a stepping motor | | [116] |
| | | Biaxial | WO 2009/032174 Al | 2009 | Tuneable elastic gel substrates are disposed in multi-well plates and a ring-shaped punch indenter applies strain to the substrate, the characteristics of which are controlled by a motor assembly coupled to a control system. Lateral and longitudinal strains may be applied to the gel | The Z-drive motor can be a stepper motor or piezoelectric actuator, a lead screw connected to the bracket, or a linear or hydraulic piston | [117] |

**Table 4** (continued)

| Frequency | Actuator type | Stress state | Patent number | Publication year | Description | Observation | Ref. |
|---|---|---|---|---|---|---|---|
| | | Biaxial | US 5,348,879 | 1994 | A flexible membrane is secured and the displacement applicator (actuated by, for example, a cam) located below the membrane deforms the membrane | | [118] |
| | | | WO 2014/165056 Al | 2014 | A linear motor is operable to move the platen to cause one or more of the pistons to apply a mechanical force to the one or more wells with which the piston is aligned | | [119] |
| | | Radial | EP 1 679 366 A1 | 2006 | Substrate holding elements move away from the centre | | [120] |
| | | Uniaxial | US 2018/0216057 Al | 2018 | A cassette device to secure and expand the material with a linear actuator is connected by an arm to a first clip holder, and the scaffold response is measurable by the force measuring component | A circuit board allows electrical stimulation | [121] |

**Table 4** (continued)

| Frequency | Actuator type | Stress state | Patent number | Publication year | Description | Observation | Ref. |
|---|---|---|---|---|---|---|---|
| | | | US 2020/0199515 Al | 2020 | A flexible platform composed of three-dimensional walls made of PDMS coated with electrically conductive films of titanium and gold serves to stimulate cells that are sitting on top of them, and their geometry and physical properties can be tailored to make them flexible (or rigid) enough to be bent by the range of forces applied by cells during contraction. One or two electrically controlled linear actuators provide reciprocating motion with a frequency of 0.5–5 Hz | Allows simultaneous electrical stimulation | [122] |
| | Magnetic actuation | Uniaxial | EP 1 428 869 A1 | 2004 | A magnetic body is attached to one end of the material and the material expands and contracts by electromagnetic force when the tensile stress is relieved | Intermittently or gradually increasing/decreasing stress generation | [123] |

**Table 4** (continued)

| Frequency | Actuator type | Stress state | Patent number | Publication year | Description | Observation | Ref. |
|---|---|---|---|---|---|---|---|
| | | | US 2008/0026419A | 2008 | An electromagnetic actuator transmits an upward directed force through a vertical piston to the culture dish, thereby providing controlled compression of a tissue sample. Loading frequency between 0.1 and 10 Hz | Confined or unconfined compression | [124] |
| | | | US 2016/0032234A1 | 2016 | Brackets attached to the flexible cell culture pool accommodate a ferromagnetic element, extending the substrate | Electrical stimulation can be applied either independently or simultaneously, by placing a pair of electrodes at two opposing sides. Several cell cultures may be stimulated by placing static magnets at the edge of each Petri dish and free magnets on the platform, which is movable by a mechanical arm coupled to a motor | [125] |
| | | | US 2021/0040427 A1 | 2021 | Actuation platforms may use magnetism to induce minute movements between a fixed portion and actuated portion (both connected by a native ECM protein upon which cells can be cultured), thus imparting tensile strain | The actuators may be a magnet or an electro-magnet, and may be made of a piezoelectric material or may be operably coupled to a hydraulic or pneumatic actuator | [126] |

**Table 4** (continued)

| Frequency | Actuator type | Stress state | Patent number | Publication year | Description | Observation | Ref. |
|---|---|---|---|---|---|---|---|
| | Fluid-flow-induced shear stress | | CN103146574A | 2013 | A negative pressure generator provides flow-shear stress and mechanical tensile force to the cell culture | | [127] |
| | | | US 8,852,923 B2 | 2014 | Fluid is passed through the passage at a Reynolds number lower than 2300 to achieve laminar flow through the passage, generating a shear stress of between 5.0 and 24 dynes/cm$^2$ | Movable and fixed anchors allow cyclic flexural and/or tensile stresses to be applied by an axial rod or axial rail, the movable one being connected to an actuator (a reciprocating motor, such as a linear motor) | [128] |
| Extremely high frequency | Piezoelectric actuator | | US 8,465,971 | 2013 | Longitudinal vibration (piezoelectric elements) is created with an external magnetic field. Frequency of vibration is 100 MHz or lower | | [129] |
| | | | WO2015167097A1 | 2014 | Ultrasonic elements create oscillation | | [130] |
| | | | US 10,260,035 B2 | 2019 | | | [131] |
| Non-conventional principles of actuation | Laser (micro-cavitation) | | US 2014/0100138A1 | 2014 | Generation of micro-cavitation bubbles using pulsed energy applies shear to cells | | [132] |
| | Environmentally responsive | | US 2015/0093823A1 | 2015 | Optically active micro-actuators allow one to fine-tune degrees and modes of tilting/bending, and local mechanical force is applied directly to cells | | [133] |

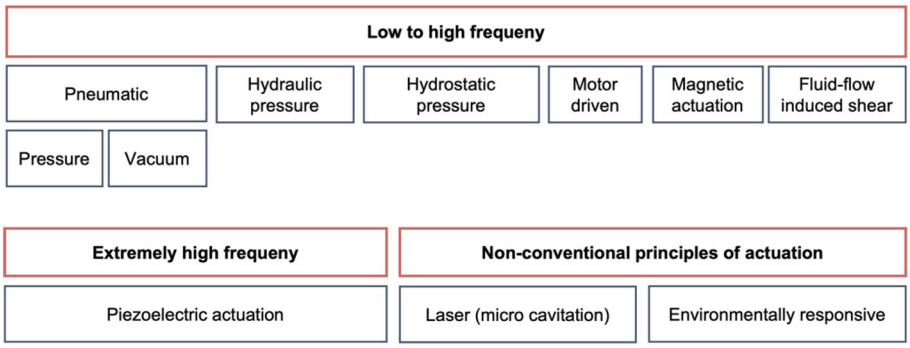


**Fig. 12** Actuation principles of various mechanical cell-stimulation devices, divided by frequency level: low to high for values up to 200 Hz and extremely high frequency for values up to 100 MHz

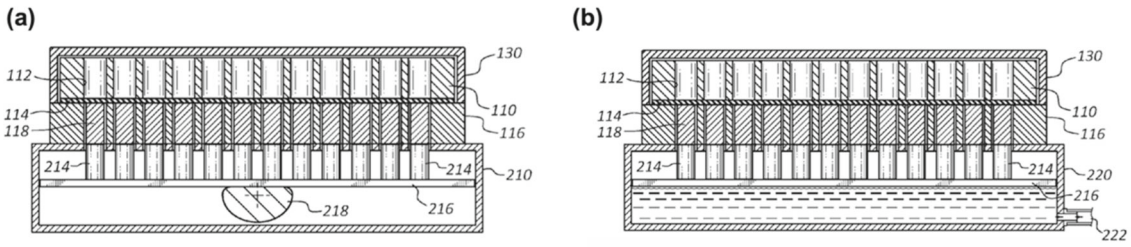


**Fig. 13** The device of invention number US 2013/0059324 AI may be operated (**a**) by a mechanical drive mechanism, in which the rotation of a non-circular shaft (218) moves the movable support (216), thereby pushing the push members (214) in respect to the pins (118); or (**b**) by a pressurized mechanism (220), in which the change of fluid volume moves the support (216), imparting mechanical strain to the cells located in the wells (112). Illustrations from [96]

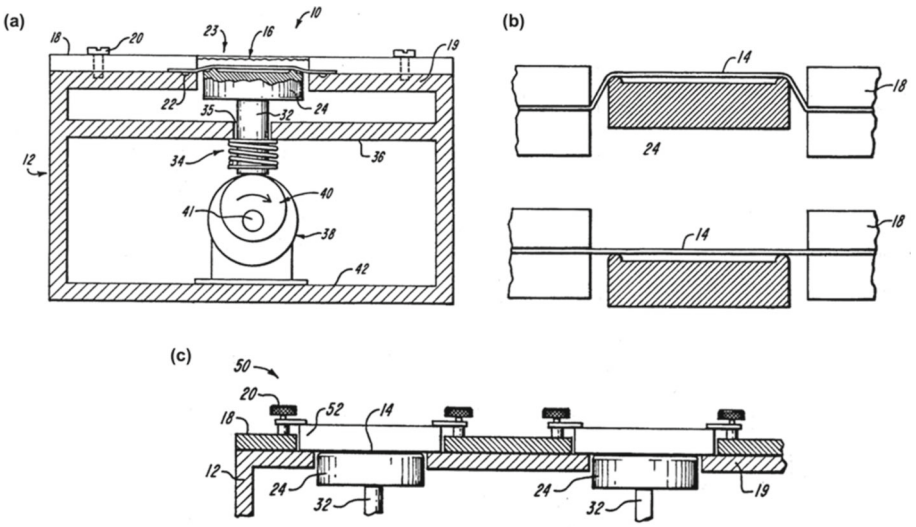


**Fig. 14** Illustrations of invention number US 5,348,879 of Shapiro et al., with three different displacement applicators (represented in the drawing by 24). In (**a**), a cam deforms the membrane, in (**b**), the membrane is secured by plates and is deformed by the displacement applicator moving upward, and in (**c**), each well is mounted above the displacement applicator. Schematics from [118]

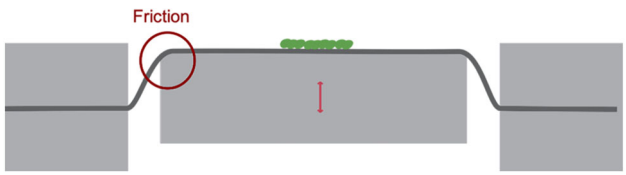


**Fig. 15** The displacement applicator moves up and down, which may create friction between the flexible membrane and the loading post

provided to enable cell culture observation by microscope and exchange of the culture medium, permitting long-term experiments to be performed.

Muthiah et al. [115] developed a mechanical tensile device, invention number US 2012/0219981Al, with dimensions of 408 mm × 150 mm (much larger than a 24-well plate). It is composed of two engagement areas located at opposite ends of a flexible substrate; each one connected to a movable element and a motor to promote opposite movements, as shown in Fig. 17. The device may include a temperature-control unit, such as a heating unit and/or a fan, to assure uniform distribution of heat and to maintain the temperature, a humidity reservoir unit, and a gas-control unit to control the gas parameters and supply. During or after tensile loading,

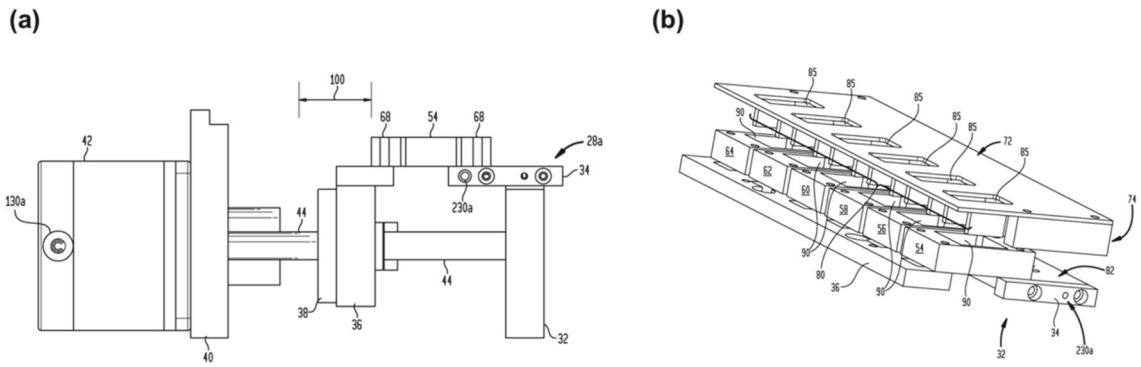


**Fig. 16** Illustrations of invention number US10,421,955B2, assigned to IonOptix LLC. (**a**) is a side view of the electromechanical stage (28a) composed by a fixed support (32) and a moving support (36) connected to a stepper motor (42). (**b**) is a perspective view illustrating six culture dishes and supporting parts of the electromechanical stage. Figures from [111]

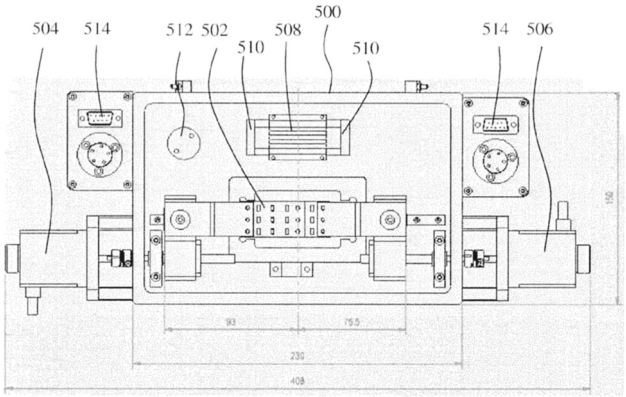


**Fig. 17** Schematics of invention number US 2012/0219981Al, assigned to Muthiah and Lane [115], in which each motor (denoted by 504 and 506) is connected to an opposite end of the cell culture device (502). The embodiment includes a water reservoir (512), an electric heating unit (508) and cooling fans (510), and computer interface connections (514). Figures from [115]

the materials may also be imaged using a microscope base plate.

The magnetic actuation principle is an indirect method used to apply mechanical stresses on the substrate of interest. The actuating part is never in contact with the moveable one, which decreases the risk of contamination, but it is hard to control the strain and velocity. In addition, there is a potential unwanted magnetic effect on cells.

Looking further at low- to high-frequency range, some inventions apply fluid-flow-induced shear stress to cells. Despite the fact that this stimulus cannot be considered a mechanical cue for mechanotransduction studies given that it cannot be measured, Jiang et al.'s invention number CN10314657A also provides, according to the inventors, tensile stresses on cells [127], and Boronyak et al.'s invention number US 8,852,923 B2 may be adapted to impose cyclic flexural and/or tensile stresses [128].

The aforementioned inventions apply tensile, compressive, or shear stresses to cells, and some allow simultaneous electric stimulation. When cells are stimulated by deformation of the substrate on which they are cultured, those forces generate uniaxial, biaxial, or equiaxial strains (previously described in Fig. 3). In-plane substrate distension through frictionless platen displacement (by vacuum, pressure, or another means) creates biaxial strain traction on a flexible culture membrane and produces a uniform strain field [119]. This strain-profile output may be required for more accurate and controlled mechanotransduction studies, given that all cells cultured on the substrate are subjected to the same strain.

Actuation using piezoelectric or ultrasound elements was used to create vibration/oscillation. The main advantage is easy set-up, but the deformation created exhibits low amplitude and high frequency. In addition, the deformation of the piezo elements is not equal to the deformation of the substrate, and consequently of the cells, because losses are always present and, as the whole device vibrates, the vibrations can be even more attenuated.

## Potential and future perspectives

Significant progress in research and technological fields has contributed to remarkable findings on the physiological dynamics of the human body. Basic life science research has moved from 2D culture systems to more complex 3D dynamic cultures, not only to improve cell culture conditions by promoting nutrient and oxygen flow to cells, but also to more closely mimic the complex physiological environment. Unlike bioreactors or microfluidic-based culture models, for the purpose of mechanobiology studies, cells are usually seeded on polymeric substrates or incorporated into 3D constructs and stimulated in mechanical force devices in order to investigate cell adaptation to different mechanical stresses, such as tensile or compressive stresses.

Regenerative medicine strategies involve the use of biomaterials whose mechanical properties and behaviour upon implantation may be studied in vitro by closely mimicking physiological conditions of, for example, bone [43, 74–76], heart muscle [42, 135], tendon [56], and lung [77]. By reproducing the physiological conditions to which the implants or biomaterials would be subjected, the need to perform in vivo animal testing would decrease. This would be in line with the European Directive 2010/63/EC which follows the "3Rs: reduction, refinement, and replacement" strategy to reinforce the importance of using alternative in vitro and in silico methods to obtain the maximal information from the intended product prior to clinical trials [136–138]. Despite more reliable studies conducted over the past years for multiple tissue-specific applications, there are still opportunities for further improvement. Mechanical stimulation devices should be designed (or integrated with other systems) to allow multiple and real-time assessment and evaluation of cell behaviour and responses at a microscale. One possibility is performing real-time imaging using non-invasive imaging techniques, fluorescence, or μCT. In order to assure optimal experimental conditions, mechanical stimulation devices could be coupled and assembled with sensors for monitor-based and cell-specific parameters, such as pH, temperature, oxygen, and secretion of small molecules and proteins.

**Acknowledgements** This work was supported by FCT (Fundação para a Ciência e a Tecnologia) through the grant SFRH/BD/141056/2018, the project PTDC/EME-EME/1442/2020 and under the national support to R&D units grant, through the reference projects UIDB/04436/2020 and UIDP/04436/2020. In addition, this work was developed within the scope of the project CICECO-Aveiro Institute of Materials, UIDB/50011/2020, UIDP/50011/2020 & LA/P/0006/2020, financed by national funds through the FCT/MEC (PIDDAC).

**Author contributions** Conceptualization: FMF, MG, GM and FSS; Methodology: FMF; Investigation: FMF; Writing – original draft: FMF; Writing – review & editing: all authors; Funding acquisition: FMF, GM and FSS; Supervision: OC, MG, GM and FSS.

**Funding** Open access funding provided by FCT|FCCN (b-on).

## Declarations

**Conflict of interest** The authors declare that they have no conflict of interest.

**Ethical approval** This article does not contain any studies with human or animal subjects performed by any of the authors.



## References

1. Roy AL, Conroy RS (2018) Toward mapping the human body at a cellular resolution. Mol Biol Cell 29:1779–1785. https://doi.org/10.1091/mbc.E18-04-0260
2. Jackson EL, Lu H (2016) Three-dimensional models for studying development and disease: moving on from organisms to organs-on-a-chip and organoids. Integr Biol 8:672–683. https://doi.org/10.1039/c6ib00039h
3. Atcha H, Davis CT, Sullivan NR et al (2018) A low-cost mechanical stretching device for uniaxial strain of cells: a platform for pedagogy in mechanobiology. J Biomech Eng 140:1–9. https://doi.org/10.1115/1.4039949
4. Raveling AR, Theodossiou SK, Schiele NR (2018) A 3D printed mechanical bioreactor for investigating mechanobiology and soft tissue mechanics. MethodsX 5:924–932. https://doi.org/10.1016/j.mex.2018.08.001
5. Yi N, Cui H, Zhang LG et al (2019) Integration of biological systems with electronic-mechanical assemblies. Acta Biomater 95:91–111. https://doi.org/10.1016/j.actbio.2019.04.032
6. Gattazzo F, Urciuolo A, Bonaldo P (2014) Extracellular matrix: a dynamic microenvironment for stem cell niche. Biochim Biophys Acta Gen Subj 1840:2506–2519. https://doi.org/10.1016/j.bbagen.2014.01.010
7. Uto K, Tsui JH, Deforest CA et al (2017) Dynamically tunable cell culture platforms for tissue engineering and mechanobiology. Prog Polym Sci 65:53–82. https://doi.org/10.1016/j.progpolymsci.2016.09.004
8. Li L, Eyckmans J, Chen CS (2017) Designer biomaterials for mechanobiology. Nat Mater 16:1164–1168. https://doi.org/10.1038/nmat5049
9. Jansen KA, Donato DM, Balcioglu HE et al (2015) A guide to mechanobiology: where biology and physics meet. Biochim Biophys Acta Mol Cell Res 1853:3043–3052. https://doi.org/10.1016/j.bbamcr.2015.05.007
10. Orr AW, Helmke BP, Blackman BR et al (2006) Mechanisms of mechanotransduction. Dev Cell 10:11–20. https://doi.org/10.1016/j.devcel.2005.12.006
11. Vining KH, Mooney DJ (2017) Mechanical forces direct stem cell behaviour in development and regeneration. Nat Rev Mol Cell Biol 18:728–742. https://doi.org/10.1038/nrm.2017.108
12. Chen Y, Ju L, Rushdi M et al (2017) Receptor-mediated cell mechanosensing. Mol Biol Cell 28:3134–3155. https://doi.org/10.1091/mbc.e17-04-0228
13. Wittkowske C, Reilly GC, Lacroix D et al (2016) In vitro bone cell models : impact of fluid shear stress on bone formation. Front Bioeng Biotechnol 4:1–22. https://doi.org/10.3389/fbioe.2016.00087
14. Ma S, Meng Z, Chen R et al (2019) The hippo pathway: biology and pathophysiology. Annu Rev Biochem 88:577–604. https://doi.org/10.1146/annurev-biochem-013118-111829
15. DuFort CC, Paszek MJ, Weaver VM (2001) Balancing forces: architectural control of mechanotransduction. Nat Rev Mol Cell Biol 12:308–319. https://doi.org/10.1038/nrm3112

16. Gasik M (2020) Biomechanical characterization of engineered tissues and implants for tissue/organ replacement applications. Biomaterials for organ and tissue regeneration. Elsevier, pp 599–627. https://doi.org/10.1016/B978-0-08-102906-0.00024-6
17. Melo-Fonseca F, Miranda G, Domingues HS et al (2020) Reengineering bone-implant interfaces for improved mechanotransduction and clinical outcomes. Stem Cell Rev Rep 16:1121–1138. https://doi.org/10.1007/s12015-020-10022-9
18. Desmaële D, Boukallel M, Régnier S (2011) Actuation means for the mechanical stimulation of living cells via microelectromechanical systems: a critical review. J Biomech 44:1433–1446. https://doi.org/10.1016/j.jbiomech.2011.02.085
19. Bhatia SN, Ingber DE (2014) Microfluidic organs-on-chips. Nat Biotechnol 32:760–772. https://doi.org/10.1038/nbt.2989
20. Adelaide Asnaghi M, Smith T, Martin I et al (2014) Bioreactors. Tissue engineering. Elsevier, pp 393–425. https://doi.org/10.1016/B978-0-12-420145-3.00012-2
21. Brunelli M, Perrault C, Lacroix D (2019) A review of bioreactors and mechanical stimuli. In: Lacroix D, Brunelli M, Perrault C et al (Eds.), Multiscale Mechanobiology in Tissue Engineering. Springer Singapore, Singapore, pp 1–22. https://doi.org/10.1007/978-981-10-8075-3_1
22. Eaker S, Abraham E, Allickson J et al (2017) Bioreactors for cell therapies: current status and future advances. Cytotherapy 19:9–18. https://doi.org/10.1016/j.jcyt.2016.09.011
23. Mckee C, Chaudhry GR (2017) Advances and challenges in stem cell culture. Colloids Surf B Biointerf 159:62–77. https://doi.org/10.1016/j.colsurfb.2017.07.051
24. Yeatts AB, Fisher JP (2011) Bone tissue engineering bioreactors: dynamic culture and the influence of shear stress. Bone 48:171–181. https://doi.org/10.1016/j.bone.2010.09.138
25. Berry JD, Godara P, Liovic P et al (2015) Predictions for optimal mitigation of paracrine inhibitory signalling in haemopoietic stem cell cultures. Stem Cell Res Ther 6:1–16. https://doi.org/10.1186/s13287-015-0048-7
26. King JA, Miller WM (2007) Bioreactor development for stem cell expansion and controlled differentiation. Curr Opin Chem Biol 11:394–398. https://doi.org/10.1016/j.cbpa.2007.05.034
27. Mazzoleni G, Di Lorenzo D, Steimberg N (2009) Modelling tissues in 3D: the next future of pharmaco-toxicology and food research? Genes Nutr 4:13–22. https://doi.org/10.1007/s12263-008-0107-0
28. Marijanovic I, Antunovic M, Matic I et al (2016) Bioreactor-based bone tissue engineering. In: Zorzi AR, Batistade Miranda J (Eds.), Advanced Techniques in Bone Regeneration. InTech. https://doi.org/10.5772/62546
29. van Noort D (2016) Bioreactors on a chip. In: Mandenius CF (Ed.), Bioreactors: Design, Operation and Novel Applications (1st Ed.). Wiley-VCH Verlag GmbH & Co, KGaA, pp 77–112
30. Sosa-Hernández JE, Villalba-Rodríguez AM, Romero-Castillo KD et al (2018) Organs-on-a-chip module: a review from the development and applications perspective. Micromachines 9:536. https://doi.org/10.3390/mi9100536
31. Whitesides GM (2006) The origins and the future of microfluidics. Nature 442:368–373. https://doi.org/10.1038/nature05058
32. Mann JM, Lam RHW, Weng S et al (2012) A silicone-based stretchable micropost array membrane for monitoring live-cell subcellular cytoskeletal response. Lab Chip 12:731–740. https://doi.org/10.1039/c2lc20896b
33. Haeberle S, Zengerle R (2007) Microfluidic platforms for lab-on-a-chip applications. Lab Chip 7:1094–1110. https://doi.org/10.1039/b706364b
34. Azizipour N, Avazpour R, Rosenzweig DH et al (2020) Evolution of biochip technology: a review from lab-on-a-chip to organ-on-a-chip. Micromachines 11:1–15. https://doi.org/10.3390/mi11060599
35. Brown TD (2000) Techniques for mechanical stimulation of cells in vitro: a review. J Biomech 33:3–14. https://doi.org/10.1016/S0021-9290(99)00177-3
36. Esteban-Manzanares G, González-Bermúdez B, Cruces J et al (2017) Improved measurement of elastic properties of cells by micropipette aspiration and its application to lymphocytes. Ann Biomed Eng 45:1375–1385. https://doi.org/10.1007/s10439-017-1795-7
37. González-Bermúdez B, Guinea GV, Plaza GR (2019) Advances in micropipette aspiration: applications in cell biomechanics, models, and extended studies. Biophys J 116:587–594. https://doi.org/10.1016/j.bpj.2019.01.004
38. Daza R, González-Bermúdez B, Cruces J et al (2019) Comparison of cell mechanical measurements provided by atomic force microscopy (AFM) and micropipette aspiration (MPA). J Mech Behav Biomed Mater 95:103–115. https://doi.org/10.1016/j.jmbbm.2019.03.031
39. Efremov YM, Wang WH, Hardy SD et al (2017) Measuring nanoscale viscoelastic parameters of cells directly from AFM force-displacement curves. Sci Rep 7:1–14. https://doi.org/10.1038/s41598-017-01784-3
40. Schierbaum N, Rheinlaender J, Schäffer TE (2019) Combined atomic force microscopy (AFM) and traction force microscopy (TFM) reveals a correlation between viscoelastic material properties and contractile prestress of living cells. Soft Matter 15:1721–1729. https://doi.org/10.1039/c8sm01585f
41. Krieg M, Fläschner G, Alsteens D et al (2019) Atomic force microscopy-based mechanobiology. Nat Rev Phys 1:41–57. https://doi.org/10.1038/s42254-018-0001-7
42. Kreutzer J, Viehrig M, Pölönen RP et al (2020) Pneumatic unidirectional cell stretching device for mechanobiological studies of cardiomyocytes. Biomech Model Mechanobiol 19:291–303. https://doi.org/10.1007/s10237-019-01211-8
43. Qi MC, Hu J, Zou SJ et al (2008) Mechanical strain induces osteogenic differentiation: Cbfa1 and Ets-1 expression in stretched rat mesenchymal stem cells. Int J Oral Maxillofac Surg 37:453–458. https://doi.org/10.1016/J.IJOM.2007.12.008
44. Trepat X, Deng L, An SS et al (2007) Universal physical responses to stretch in the living cell. Nature 447:592–595. https://doi.org/10.1038/nature05824
45. Sniadecki NJ, Anguelouch A, Yang MT et al (2007) Magnetic microposts as an approach to apply forces to living cells. Proc Natl Acad Sci USA 104:14553–14558. https://doi.org/10.1073/pnas.0611613104
46. Izzo L, Tunesi M, Boeri L et al (2019) Influence of the static magnetic field on cell response in a miniaturized optically accessible bioreactor for 3D cell culture. Biomed Microdev 21:1–12. https://doi.org/10.1007/s10544-019-0387-8
47. Heidemann SR, Wirtz D (2004) Towards a regional approach to cell mechanics. Trends Cell Biol 14:160–166. https://doi.org/10.1016/j.tcb.2004.02.003
48. Barthes J, Özçelik H, Hindié M et al (2014) Cell microenvironment engineering and monitoring for tissue engineering and regenerative medicine: the recent advances. Biomed Res Int 2014:921905. https://doi.org/10.1155/2014/921905
49. Halldorsson S, Lucumi E, Gómez-Sjöberg R et al (2015) Advantages and challenges of microfluidic cell culture in polydimethylsiloxane devices. Biosens Bioelectron 63:218–231. https://doi.org/10.1016/j.bios.2014.07.029
50. Kim L, Toh YC, Voldman J et al (2007) A practical guide to microfluidic perfusion culture of adherent mammalian cells. Lab Chip 7:681–694. https://doi.org/10.1039/b704602b
51. Kluge JA, Leisk GG, Cardwell RD et al (2011) Bioreactor system using noninvasive imaging and mechanical stretch for biomaterial screening. Ann Biomed Eng 39:1390–1402. https://doi.org/10.1007/s10439-010-0243-8

52. Walker M, Godin M, Pelling AE (2018) A vacuum-actuated microtissue stretcher for long-term exposure to oscillatory strain within a 3D matrix. Biomed Microdev 20(2):1–10. https://doi.org/10.1007/s10544-018-0286-4
53. Vanderploeg EJ, Imler SM, Brodkin KR et al (2004) Oscillatory tension differentially modulates matrix metabolism and cytoskeletal organization in chondrocytes and fibrochondrocytes. J Biomech 37:1941–1952. https://doi.org/10.1016/j.jbiomech.2004.02.048
54. Connelly JT, Vanderploeg EJ, Mouw JK et al (2010) Tensile loading modulates bone marrow stromal cell differentiation and the development of engineered fibrocartilage constructs. Tissue Eng Part A 16:1913–1923. https://doi.org/10.1089/ten.tea.2009.0561
55. Doroski DM, Levenston ME, Temenoff JS (2010) Cyclic tensile culture promotes fibroblastic differentiation of marrow stromal cells encapsulated in poly(ethylene glycol)-based hydrogels. Tissue Eng Part A 16:3457–3466. https://doi.org/10.1089/ten.tea.2010.0233
56. Grier WK, Moy AS, Harley BAC (2017) Cyclic tensile strain enhances human mesenchymal stem cell SMAD 2/3 activation and tenogenic differentiation in anisotropic collagen-glycosaminoglycan scaffolds. Eur Cells Mater 33:227–239. https://doi.org/10.22203/eCM.v033a14
57. Subramanian G, Elsaadany M, Bialorucki C et al (2017) Creating homogenous strain distribution within 3D cell-encapsulated constructs using a simple and cost-effective uniaxial tensile bioreactor: design and validation study. Biotechnol Bioeng 114:1878–1887. https://doi.org/10.1002/bit.26304
58. Ralphs JR, Waggett AD, Benjamin M (2002) Actin stress fibres and cell–cell adhesion molecules in tendons: organisation in vivo and response to mechanical loading of tendon cells in vitro. Matrix Biol 21:67–74. https://doi.org/10.1016/S0945-053X(01)00179-2
59. Simmons CA, Matlis S, Thornton AJ et al (2003) Cyclic strain enhances matrix mineralization by adult human mesenchymal stem cells via the extracellular signal-regulated kinase (ERK1/2) signaling pathway. J Biomech 36:1087–1096. https://doi.org/10.1016/S0021-9290(03)00110-6
60. Sumanasinghe RD, Bernacki SH, Loboa EG (2006) Osteogenic differentiation of human mesenchymal stem cells in collagen matrices: effect of uniaxial cyclic tensile strain on bone morphogenetic protein (BMP-2) mRNA expression. Tissue Eng 12:3459–3465. https://doi.org/10.1089/ten.2006.12.3459
61. Saha S, Ji L, De Pablo JJ et al (2006) Inhibition of human embryonic stem cell differentiation by mechanical strain. J Cell Physiol 206:126–137. https://doi.org/10.1529/biophysj.107.119891
62. Ku CH, Johnson PH, Batten P et al (2006) Collagen synthesis by mesenchymal stem cells and aortic valve interstitial cells in response to mechanical stretch. Cardiovasc Res 71:548–556. https://doi.org/10.1016/j.cardiores.2006.03.022
63. Luo J, Qin L, Zhao L et al (2020) Tissue-engineered vascular grafts with advanced mechanical strength from human iPSCs. Cell Stem Cell 26:251–261. https://doi.org/10.1016/j.stem.2019.12.012
64. Kroll K, Chabria M, Wang K et al (2017) Electro-mechanical conditioning of human iPSC-derived cardiomyocytes for translational research. Prog Biophys Mol Biol 130:212–222. https://doi.org/10.1016/j.pbiomolbio.2017.07.003
65. Sitticholechaiwut A, Edwards JH, Scutt AM et al (2010) Short bouts of mechanical loading are as effective as dexamethasone at inducing matrix production by human bone marrow mesenchymal stem cells. Eur Cells Mater 20:45–57. https://doi.org/10.22203/eCM.v020a05
66. Sittichockechaiwut A, Scutt AM, Ryan AJ et al (2009) Use of rapidly mineralising osteoblasts and short periods of mechanical loading to accelerate matrix maturation in 3D scaffolds. Bone 44:822–829. https://doi.org/10.1016/j.bone.2008.12.027
67. Kong Z, Li J, Zhao Q et al (2012) Dynamic compression promotes proliferation and neovascular networks of endothelial progenitor cells in demineralized bone matrix scaffold seed. J Appl Physiol 113:619–626. https://doi.org/10.1152/japplphysiol.00378.2011
68. Okazaki Y, Furumatsu T, Kamatsuki Y et al (2021) Differences between the root and horn cells of the human medial meniscus from the osteoarthritic knee in cellular characteristics and responses to mechanical stress. J Orthop Sci 26:230–236. https://doi.org/10.1016/j.jos.2020.02.015
69. Chang SH, Mori D, Kobayashi H et al (2019) Excessive mechanical loading promotes osteoarthritis through the gremlin-1–NF-κB pathway. Nat Commun 10:1–5. https://doi.org/10.1038/s41467-019-09491-5
70. Nam HY, Murali MR, Ahmad RE et al (2020) Mechanical strain-mediated tenogenic differentiation of mesenchymal stromal cells is regulated through epithelial sodium channels. Stem Cells Int 2020:5385960. https://doi.org/10.1155/2020/5385960
71. Takahashi K, Ito S, Furuya K et al (2017) Real-time imaging of mechanically and chemically induced ATP release in human lung fibroblasts. Respir Physiol Neurobiol 242:96–101. https://doi.org/10.1016/j.resp.2017.04.008
72. Kamotani Y, Bersano-Begey T, Kato N et al (2008) Individually programmable cell stretching microwell arrays actuated by a Braille display. Biomaterials 29:2646–2655. https://doi.org/10.1016/j.biomaterials.2008.02.019
73. Gere JM, Timoshenko SP (1984) Mechanics of Materials (2nd Ed.). Brooks/Cole Engineering, Escondido
74. Mauney JR, Sjostorm S, Blumberg J et al (2004) Mechanical stimulation promotes osteogenic differentiation of human bone marrow stromal cells on 3-D partially demineralized bone scaffolds in vitro. Calcif Tissue Int 74:458–468. https://doi.org/10.1007/s00223-003-0104-7
75. Byrne EM, Farrell E, McMahon LA et al (2008) Gene expression by marrow stromal cells in a porous collagen–glycosaminogly scaffold is affected by pore size and mechanical stimulation. J Mater Sci Mater Med 19:3455–3463. https://doi.org/10.1007/s10856-008-3506-2
76. Jagodzinski M, Drescher M, Zeichen J et al (2004) Effects of cyclic longitudinal mechanical strain and dexamethasone on osteogenic differentiation of human bone marrow stromal cells. Eur Cells Mater 7:35–41. https://doi.org/10.22203/eCM.v007a04
77. Huh D, Matthews BD, Mammoto A et al (2010) Reconstituting organ-level lung functions on a chip. Science 328(5986):1662–1668. https://doi.org/10.1126/science.1188302
78. Butcher JT, Barrett BC, Nerem RM (2006) Equibiaxial strain stimulates fibroblastic phenotype shift in smooth muscle cells in an engineered tissue model of the aortic wall. Biomaterials 27:5252–5258. https://doi.org/10.1016/j.biomaterials.2006.05.040
79. Moraes C, Chen JH, Sun Y et al (2010) Microfabricated arrays for high-throughput screening of cellular response to cyclic substrate deformation. Lab Chip 10:227–234. https://doi.org/10.1039/b914460a
80. Tan W, Scott D, Belchenko D et al (2008) Development and evaluation of microdevices for studying anisotropic biaxial cyclic stretch on cells. Biomed Microdev 10:869–882. https://doi.org/10.1007/s10544-008-9201-8
81. Gould RA, Chin K, Santisakultarm TP et al (2012) Cyclic strain anisotropy regulates valvular interstitial cell phenotype and tissue remodeling in three-dimensional culture. Acta Biomater 8:1710–1719. https://doi.org/10.1016/j.actbio.2012.01.006
82. Terraciano V, Mizrahi J, Moroni L et al (2007) Differential response of adult and embryonic mesenchymal progenitor cells to mechanical compression in hydrogels. Stem Cells 25:2730–2738. https://doi.org/10.1634/stemcells.2007-0228

83. Mouw JK, Connelly JT, Wilson CG et al (2006) Dynamic compression regulates the expression and synthesis of chondrocyte-specific matrix molecules in bone marrow stromal cells. Stem Cells 25:655–663. https://doi.org/10.1634/stemcells.2006-0435
84. Rath B, Nam J, Knobloch TJ et al (2008) Compressive forces induce osteogenic gene expression in calvarial osteoblasts. J Biomech 41:1095–1103. https://doi.org/10.1016/j.jbiomech.2007.11.024
85. Ravichandran A, Lim J, Chong MSK et al (2017) In vitro cyclic compressive loads potentiate early osteogenic events in engineered bone tissue. J Biomed Mater Res Part B Appl Biomater 105:2366–2375. https://doi.org/10.1002/jbm.b.33772
86. Moraes C, Wang GH, Sun Y et al (2010) A microfabricated platform for high-throughput unconfined compression of micropatterned biomaterial arrays. Biomaterials 31:577–584. https://doi.org/10.1016/j.biomaterials.2009.09.068
87. Lee D, Erickson A, You T et al (2018) Pneumatic microfluidic cell compression device for high-throughput study of chondrocyte mechanobiology. Lab Chip 18:2077–2086. https://doi.org/10.1039/c8lc00320c
88. Moraes C, Zhao R, Likhitpanichkul M et al (2011) Semi-confined compression of microfabricated polymerized biomaterial constructs. J Micromech Microeng 21:054014. https://doi.org/10.1088/0960-1317/21/5/054014
89. Zhang ZZ, Chen YR, Wang SJ et al (2019) Orchestrated biomechanical, structural, and biochemical stimuli for engineering anisotropic meniscus. Sci Transl Med 11:eaao0750. https://doi.org/10.1126/scitranslmed.aao0750
90. Analytics C Web of Knowledge—Derwent Innovation Index. http://www.webofknowledge.com
91. Google Patents. https://patents.google.com
92. Moraes C, Simmons C, Sun Y (2009) A system, apparatus and method for applying mechanical force to a material (Patent No. WO2009039640A9). https://patents.google.com/patent/WO2009039640A1/en
93. Banes AJ (1989) Apparatus for applying stress to cell cultures (Patent No. US4839280). https://patents.google.com/patent/US4839280?oq=US4839280
94. Tae Yoon L, Hee Tak H, Jung Mok S et al (2019) Cell stimulation apparatus (Patent No. US 10,246,676 B2). https://patents.google.com/patent/US10246676B2
95. Banes AJ (2002) Loading station assembly and method for tissue engineering (Patent No. US 6,472,202 Bl). https://patents.google.com/patent/US6472202B1/en
96. Sittampalam GS, Nirmalanandhan VS (2013) Systems and methods for mechanically strained cell culture (Patent No. US 2013/0059324 Al). https://patents.google.com/patent/US20130059324A1/en
97. Simmons CS, Pruitt BL, Sim JY et al (2015) Cell culture strain array systems and methods for using the same (Patent No. US2015/0050722Al). https://patents.google.com/patent/US20150050722A1/en
98. Kiesow A, Schwan S, Bartling B et al (2011) Bioreactor for multi-dimensional, mechanical stimulation of cells, cell complexes and/or cell tissue, comprises a first and a second reactor part volumes that are separated from each other through a carrier membrane (Patent No. DE102009057698A1). https://patents.google.com/patent/DE102009057698A1/de
99. Min-Hsien W, Chun-Li L, Shiao-Wen T et al (2015) Apparatus for high-throughput cell culture with mechanical compression stimulation (Patent No. US 8980624 B2). https://patents.google.com/patent/US8980624B2/en
100. Kasra M (2016) Hydrostatic pressure generator device (Patent No. US 9303244 Bl). https://patents.google.com/patent/US9303244B1/en
101. Dan-Jae L, Ming-Tzu T, Chao-Wei H et al (2020) Cell mechanical stimulating device (Patent No. US 2020/0339936 Al). https://patents.google.com/patent/US20200339936A1/en
102. Lagana K, Raimondi MT, Dubini G et al (2009) Bioreactor for generation and complex mechanical stimulation of engineered biological tissue (Patent No. WO 2009/047045 A2). https://patents.google.com/patent/WO2009047045A2/en
103. Wang BC, Zhu LQ, Zhou J et al (2006) Microstress applicator for in vitro cell (Patent No. CN1834220A). https://patents.google.com/patent/CN1834220A/en
104. Subramanian G, Elsaadany M, Yildirim-Ayan E (2017) Loading platform for three-dimensional tissue engineered scaffolds (Patent No. CN1834220A). https://patents.google.com/patent/CN1834220A/en
105. Franck C, Bar-kochba E (2013) Device and system for mechanical measurement of biomaterial (Patent No. WO 2013/090738 A9). https://patents.google.com/patent/WO2013090738A9/en
106. Fan YB, Li JC, Zou YW et al (2008) Tissue engineering reactor having tissue cultures tension-compression and rotation functions (Patent No. CN101372664A). https://patents.google.com/patent/CN101372664A/en
107. Fan YB, Li P, Liu ML et al (2012) Stretch-electricity combined stimulation three-dimensional cell culture device (Patent No. CN102433258B). https://patents.google.com/patent/CN102433258B/en
108. Zhang B, Feng ZQ, Wang QF et al (2014) Culture device applied to cell tensile stress and method (Patent No. CN103966094A). https://patents.google.com/patent/CN103966094A/en
109. Lu HH, Castillo M, Dargis BR (2012) Bioreactor system for mechanical stimulation of biological samples (Patent No. US 2012/0100602 Al). https://patents.google.com/patent/US20120100602A1/en
110. Lee PGW, Tillostson DL, Udale RT et al (2017) Apparatus and method for culturing cells and tissue (Patent No. US 9617507 B2). https://patents.google.com/patent/US9617507B2/en
111. Lee PGW, Tillostson DL, Udale RT et al (2019) Apparatus and method for culturing cells and tissue (Patent No. US 10,421,955 B2). https://patents.google.com/patent/US10421955B2/en
112. Meckel T, Sapper E, Schmitt LA (2018) Testing arrangement for examining a cell culture under the effect of a dynamic force (Patent No. US20180164278A1). https://patents.google.com/patent/US20180164278A1/en
113. Biagiotti L, Cavalcanti S, Giordano E et al (2011) Bio reactor for stem cells stimulation (Patent No. WO 2011/013067 A2). https://patents.google.com/patent/WO2011013067A2/en
114. Bayés Genís A, Llucià Valldeperas A, Soler Botija C et al (2017) Method for conditioning stem cells (Patent No. WO 2017/125159 Al). https://patents.google.com/patent/WO2017125159A1/en
115. Muthiah M, Lane EB (2012) Mechanical stretching device (Patent No. US 2012/0219981 Al). https://patents.google.com/patent/US20120219981A1/en
116. Jing H, Qin YX, Hai T et al (2009) Extension and compression device of multi-unit cells (Patent No. CN101649291A). https://patents.google.com/patent/CN101649291A/en
117. Krishnan R, Park CY, Tschumperlin D et al (2008) Bio-matrix stretcher (Patent No. WO 2009/032174 Al). https://patents.google.com/patent/WO2009032174A1/en
118. Shapiro AR, Gray ML, Melendez LA et al (1994) Cell stretching method (Patent No. US 5,348,879). https://patents.google.com/patent/US5348879A/en
119. Baker A, Wong M (2014) High-throughput mechanical strain generating system for cell cultures and applications thereof (Patent No. WO 2014/165056 Al). https://patents.google.com/patent/WO2014165056A1/en

120. Quinn T, Majd H (2006) Device for cell culture on deformable surfaces (Patent No. EP 1 679 366 A1).
121. Campbell S, Schwan J, Kwaczala A et al (2018) System and method for generating biological tissue (Patent No. US 2018/0216057 Al). https://patents.google.com/patent/US20180216057A1/en
122. Roberts EG (2020) Flexible device and its application for bio-cell in-vitro electrical and mechanical stimulation characterization (Patent No. US 2020/0199515 Al). https://patents.google.com/patent/US20200199515A1/en
123. Takagi T, Watanabe S (2004) Cell and structure incubator (Patent No. EP 1 428 869 A1).
124. Bottlang M, Sommers MB (2008) Method and systems for tissue culture (Patent No. US2008/0026419A). https://patents.google.com/patent/US20080026419A1/en
125. Rosell Ferrer FX, Sánchez Terrones B, Bragós Bardia R et al (2016) Methods and devices for mechanical and electrical stimulation of stem cell monolayer and 3D cultures for tissue engineering applications (Patent No. US 2016/0032234A1). https://patents.google.com/patent/US20160032234A1/en
126. Lee H, Park H, Solorio L et al (2021) High-throughput magnetic actuation platform for cancer treatment screening (Patent No. US 2021/0040427 Al). https://patents.google.com/patent/US20210040427A1/en
127. Jiang XY, Zheng WF, Zhang W et al (2013) High-flux microfluidic biomechanical long-term stimulation system and use thereof (Patent No. CN103146574A). https://patents.google.com/patent/CN103146574A/en
128. Boronyak SM, Engelmayr GC, Ramaswamy S et al (2014) Flow-stretch-flexure bioreactor (Patent No. US 8,852,923 B2). https://patents.google.com/patent/US8852923B2/en
129. Kishida A, Furunzono T, Miyazaki K et al (2013) Method for controlling biological function with mechanical vibration and device therefor (Patent No. US 8465971). https://patents.google.com/patent/US8465971B2/en
130. Choi HS, Lee WJ, Jung JT (2015) Cell stimulating system (Patent No. WO2015167097A1). https://patents.google.com/patent/WO2015167097A1/en
131. Choi HS, Lee WJ, Jung JT (2019) Cell stimulating system (Patent No. US 10,260,035 B2). https://patents.google.com/patent/US10260035B2/en
132. Botvinick EL, Venugopalan V, Compton J et al (2014) Mechanical stress response analysis of cells and tissues (Patent No. US 2014/0100138A1). https://patents.google.com/patent/US20140100138A1/en
133. Sutton AA, Shirman T, Aizenberg J et al (2015) Environmentally responsive microstructured hybrid actuator assemblies for use in mechanical stimulation of cells (Patent No. US 2015/0093823Al). https://patents.google.com/patent/US20150093823A1/en
134. Zhang W, Huang G, Xu F (2020) Engineering biomaterials and approaches for mechanical stretching of cells in three dimensions. Front Bioeng Biotechnol 8:1–14. https://doi.org/10.3389/fbioe.2020.589590
135. Birla RK, Huang YC, Dennis RG (2007) Development of a novel bioreactor for the mechanical loading of tissue-engineered heart muscle. Tissue Eng 13:2239–2248. https://doi.org/10.1089/ten.2006.0359
136. Gasik M (2017) Understanding biomaterial-tissue interface quality: combined in vitro evaluation. Sci Technol Adv Mater 18:550–562. https://doi.org/10.1080/14686996.2017.1348872
137. Patronek GJ, Rauch A (2007) Systematic review of comparative studies examining alternatives to the harmful use of animals in biomedical education. J Am Vet Med Assoc 230:37–43. https://doi.org/10.2460/javma.230.1.37
138. Reifenrath J, Angrisani N, Lalk M et al (2014) Replacement, refinement, and reduction: necessity of standardization and computational models for long bone fracture repair in animals. J Biomed Mater Res Part A 102:2884–2900. https://doi.org/10.1002/jbm.a.34920

## Authors and Affiliations

**F. Melo-Fonseca[1,2,3] · O. Carvalho[1,2] · M. Gasik[4,5] · G. Miranda[6] · F. S. Silva[1,2]**

1 Center for MicroElectroMechanical Systems, University of Minho (CMEMS-UMinho), Campus de Azurém, 4800-058 Guimarães, Portugal

2 LABBELS –Associate Laboratory, Braga, Guimarães, Portugal

3 International Iberian Nanotechnology Laboratory (INL), 4715-330 Braga, Portugal

4 School of Chemical Engineering, Aalto University Foundation, 00076 Espoo, Finland

5 Seqvera Ltd., Helsinki, Finland

6 Department of Materials and Ceramic Engineering, CICECO, Aveiro Institute of Materials, University of Aveiro, 3810-193 Aveiro, Portugal